

**A STUDY OF TOTAL INTERNAL REFLECTION SYSTEM FOR
BIOMOLECULAR INTERACTION MONITORING**



**A THESIS SUBMITTED IN PARTIAL FULFILLMENT
OF THE REQUIREMENTS FOR
THE DEGREE OF MASTER OF ENGINEERING
(BIOMEDICAL ENGINEERING)
FACULTY OF GRADUATE STUDIES
MAHIDOL UNIVERSITY**

2005

ISBN 974-04-5887-4

COPYRIGHT OF MAHIDOL UNIVERSITY

Thesis
Entitled

**A STUDY OF TOTAL INTERNAL REFLECTION SYSTEM FOR
BIOMOLECULAR INTERACTION MONITORING**



Chotchawal Wongmahasiri

Mr.Chotchawal Wongmahasiri
Candidate

Cham Promptmas

Asst.Prof.Chamras Promptmas,
Ph.D.(Biochemistry)
Major-Advisor

Warakorn Charoensuk

Asst.Prof.Warakorn Charoensuk,
Ph.D.(Electrical Engineering)
Co-Advisor

Rassmidara Hoonsawat

Assoc.Prof.Rassmidara Hoonsawat,
Ph.D.
Dean
Faculty of Graduate Studies

Theeraporn Rubcumintara

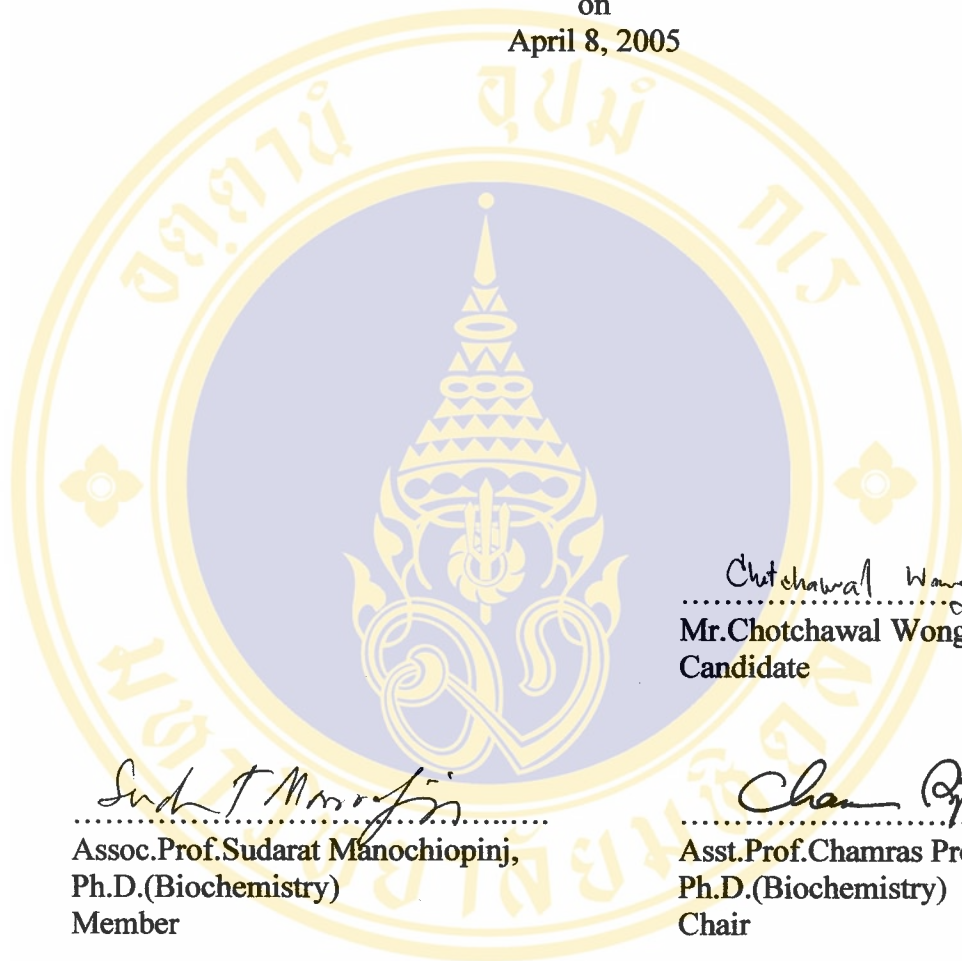
Asst.Prof.Theeraporn Rubcumintara,
Ph.D.(Materials Engineering & Science)
Chair
Master of Engineering Program in
Biomedical Engineering
Faculty of Engineering

Thesis
Entitled

**A STUDY OF TOTAL INTERNAL REFLECTION SYSTEM FOR
BIOMOLECULAR INTERACTION MONITORING**

was submitted to the Faculty of Graduate Studies, Mahidol University
for the degree of Master of Engineering (Biomedical Engineering)

on
April 8, 2005



Chotchawal Wongmahasiri

Mr.Chotchawal Wongmahasiri
Candidate

Sudarut Manochiopinij

Assoc.Prof.Sudarut Manochiopinij,
Ph.D.(Biochemistry)
Member

Chamras Promptmas

Asst.Prof.Chamras Promptmas,
Ph.D.(Biochemistry)
Chair

Udom Tipayamontri

Asst.Prof.Udom Tipayamontri,
Ph.D.(Physiology)
Member

Warakorn Charoensuk

Asst.Prof.Warakorn Charoensuk,
Ph.D.(Electrical Engineering)
Member

Rassmidara Hoonsawat

Assoc.Prof.Rassmidara Hoonsawat,
Ph.D.
Dean
Faculty of Graduate Studies
Mahidol University

Piya Ratanasuwan

Asst.Prof.Piya Ratanasuwan,
M.Eng.
Dean
Faculty of Engineering
Mahidol University

ACKNOWLEDGEMENT

For the successful of this thesis, I would like to thank Assist. Prof. Chamras Promptmas and Assist. Prof. Warakorn Charoensuk, my major-advisor and co-advisor respectively, for their support and assistance. I deeply thank them for their valuable advice and guidance in this research.

I deeply thank Dr. Boonsong Sutapun, Chief of the Electro-Optic Section of National Electronics and Computer Technology Center (NECTEC), for kindness in providing all optical instruments and instructing all related theories and techniques required.

I sincerely thank all researchers and assistant researchers of Electro-Optics Section of National Electronics and Computer Technology Center, especially Armote Somboonkaew and Ratasart Umarit, for their kindness in providing many valuable suggestions for system design and development. Without their help, this could not have been possible.

I would like to thank Peangpim Burivong, Pornpimon Punteeranurak, for their kindness in providing many kinds of solution and immobilization of sensor chip. Especially Palakorn Tantilipikara, I wish to thank you for all consultations.

Finally, I am grateful to my family for their financial support and entirely care. The usefulness of this thesis, I dedicate to my father and my mother.

Chotchawal Wongmahasiri

A STUDY OF TOTAL INTERNAL REFLECTION SYSTEM FOR
BIOMOLECULAR INTERACTION MONITORING.

CHOTCHAWAL WONGMAHASIRI 4337544 EGBE/M

M.Eng. (BIOMEDICAL ENGINEERING)

THESIS ADVISOR: CHAMRAS PROMPTMAS, Ph.D, WARAKORN
CHAROENSUK, Ph.D.

ABSTRACT

The evanescent wave is an electromagnetic wave which is generated from the total internal reflection of light. In many types of biosensor, such as fluorescent immunosensors, the evanescent wave has been used along with other techniques for monitoring biomolecular interactions.

In this thesis, a system using evanescent wave generated by the total internal reflection of light was developed for biomolecular interaction monitoring. A 635 nm laser diode was used as the laser source. The laser beam was resized by a set of lenses before passing through the sensor chip. The evanescent wave was produced by the total internal reflection of the laser beam. Cyanine 5 labeled albumin was used as a model for simulating the interaction of biomolecules. Cyanine 5 labeled albumin with concentrations ranging from undiluted, 1:4, 1:16, 1:32, 1:64, 1:128, and blank were directly immobilized on the sensor chip. Fluorescence excited by the evanescent wave was collected and filtered by another set of lenses and interference filter, respectively, before passing through the photomultiplier tube. The signal was then converted to an electrical signal and displayed by digital multimeter. The end-point voltage level of the signal in each concentration were 0.54 V, 0.46 V, 0.41 V, 0.28 V, 0.18 V, 0.12 V and 0.015 V, respectively. The data indicates that this system can detect Cyanine 5 labeled albumin at the lowest concentration of 8 $\mu\text{g/ml}$.

KEY WORDS : TOTAL INTERNAL REFLECTION, EVANESCENCE,
FLUORESCENCE.

64 P. ISBN. 974-04-5887-4

การศึกษาระบบสะท้อนแสงกลับหมดสำหรับการติดตามปฏิกิริยาชีวโมเลกุล
(A STUDY OF TOTAL INTERNAL REFLECTION SYSTEM FOR
BIOMOLECULAR INTERACTION MONITORING)

โชติชวาล วงศ์มหาศิริ 4337544 EGBE/M

วศ.ม (วิศวกรรมชีวการแพทย์)

คณะกรรมการควบคุมวิทยานิพนธ์: จำรัส พร้อมมาศ, Ph.D, วรากร เจริญสุข, Ph.D.

บทคัดย่อ

คลื่นหายตัวอย่างรวดเร็วเป็นคลื่นแม่เหล็กไฟฟ้าที่เกิดจากการสะท้อนกลับหมดของแสงในไบโอเซนเซอร์หลายชนิด ตัวอย่างเช่น ฟลูออเรสเซนต์อิมมูโนเซนเซอร์ ได้ใช้คลื่นหายตัวอย่างรวดเร็วร่วมกับเทคนิคอื่นๆ เพื่อติดตามปฏิกิริยาชีวโมเลกุล

การออกแบบระบบสะท้อนแสงกลับหมดสำหรับการติดตามปฏิกิริยาชีวโมเลกุลในวิทยานิพนธ์นี้มีการใช้เลเซอร์ไดโอดที่มีความยาวคลื่น 635 นาโนเมตรเป็นแหล่งกำเนิดแสงเลเซอร์ ซึ่งส่องผ่านชุดเลนส์เพื่อปรับขนาดของลำแสงก่อนเข้าสู่เซนเซอร์ชิฟและใช้โปรตีนอัลบูมินที่ติดฉลากด้วยสารเรืองแสงที่ความเข้มข้นเริ่มต้นจาก ไม่เจือจาง, 1:4, 1:16, 1:32, 1:64, 1:128, และ ไม่มีอัลบูมินที่ติดฉลากด้วยสารเรืองแสง ตรึงลงบนผิวของเซนเซอร์ชิฟเป็นแบบจำลองในการทดลอง แล้วทำการวัดค่าการเรืองแสงของโมเลกุลสารเรืองแสงที่ถูกกระตุ้นโดยคลื่นหายตัวอย่างรวดเร็ว ซึ่งจะผ่านการกรองก่อนส่งผ่านไปยังหลอดโฟโตมัลติพลายเออร์เพื่อแปลงเป็นสัญญาณทางไฟฟ้า พบว่าค่าระดับความต่างศักย์ที่จุดสุดท้ายของแต่ละความเข้มข้นเท่ากับ 0.54 โวลต์, 0.46 โวลต์, 0.41 โวลต์, 0.28 โวลต์, 0.18 โวลต์, 0.12 โวลต์ และ 0.015 โวลต์ ตามลำดับ นอกจากนี้ยังพบว่าระบบที่ออกแบบขึ้นสามารถตรวจวัดโปรตีนอัลบูมินที่ติดฉลากด้วยสารเรืองแสงที่ความเข้มข้นต่ำสุดประมาณ 8 ไมโครกรัมต่อมิลลิลิตร

64 หน้า ISBN. 974-04-5887-4

CONTENTS

	Page
ACKNOWLEDGEMENT	iii
ABSTRACT	iv
LIST OF FIGURES	ix
LIST OF ABBREVIATIONS	xi
CHAPTER	
I. INTRODUCTION	1
1.1 Background	1
1.2 Objective	2
II. LITERATURE REVIEW	3
2.1 Theory	3
2.1.1 Total internal reflection and evanescent wave	3
2.1.2 Fluorescence	8
2.1.3 Lock-in Amplifier	9
2.1.4 Photomultiplier Tube	12
2.1.4.1 Construction	13
2.1.4.2 Electron multiplier	14
2.1.4.3 Spectral response	18
2.1.4.4 Photocathode material	18
2.1.5 Laser source	19
2.1.5.1 The element of laser	20
2.1.5.2 Lasing process	21
2.1.5.3 Type of laser	22
2.2 Related work	23
2.2.1 Surface plasmon resonance (SPR)	23
2.2.2 Total internal reflection fluorescence	24

CONTENTS

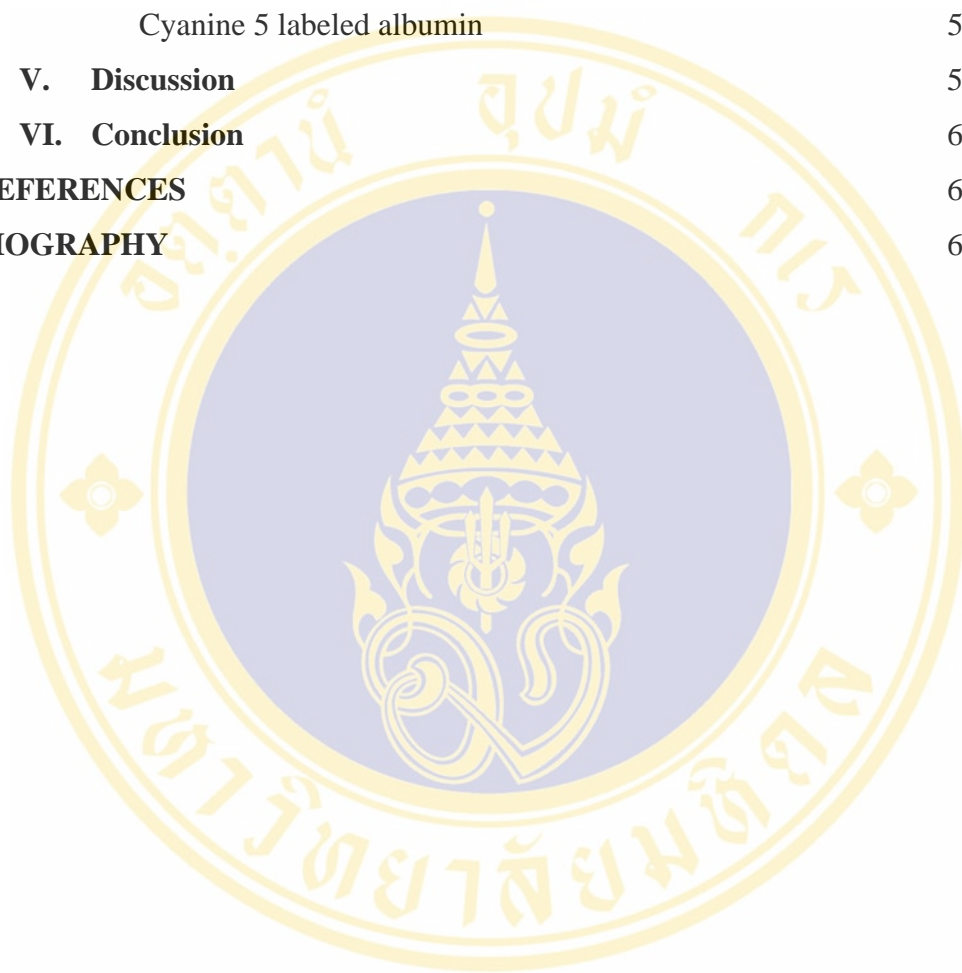
(Continued)

	Page
2.2.3 Grating coupler	28
III. MATERIALS AND METHODS	29
3.1 Materials	29
3.1.1 Chemicals	29
3.1.2 Optical equipments	29
3.1.3 Sensor chip and design	29
3.1.4 Electronic devices	30
3.2 Methods	30
3.2.1 Calculation	30
3.2.2 Sample preparation	31
3.2.2.1 The Cyanine 5 solution	31
3.2.2.2 Labeling process	31
3.2.3 Immobilization of Cyanine 5 labeled albumin on sensor chip	31
3.2.4 Set up for fluorescence detection	32
3.2.5 System testing	33
3.2.6 Negative control	34
3.2.7 Surface specific testing	34
3.2.8 Error correction	35
IV. RESULTS	36
4.1 The critical angle calculation	36
4.2 The spectrum of excitation and fluorescence	37
4.3 Stability of fluorescent signal	39
4.4 Response of the system set up to various concentration of Cyanine 5 solution in PBS	41
4.5 Immobilized sensor chip	44
4.6 Negative control	46
4.7 Surface specific testing	48
4.8 Error and correction	50

CONTENTS

(Continued)

	Page
4.9 Response of the developed system to various dilution of Cyanine 5 labeled albumin	53
V. Discussion	56
VI. Conclusion	60
REFERENCES	61
BIOGRAPHY	64



LIST OF FIGURES

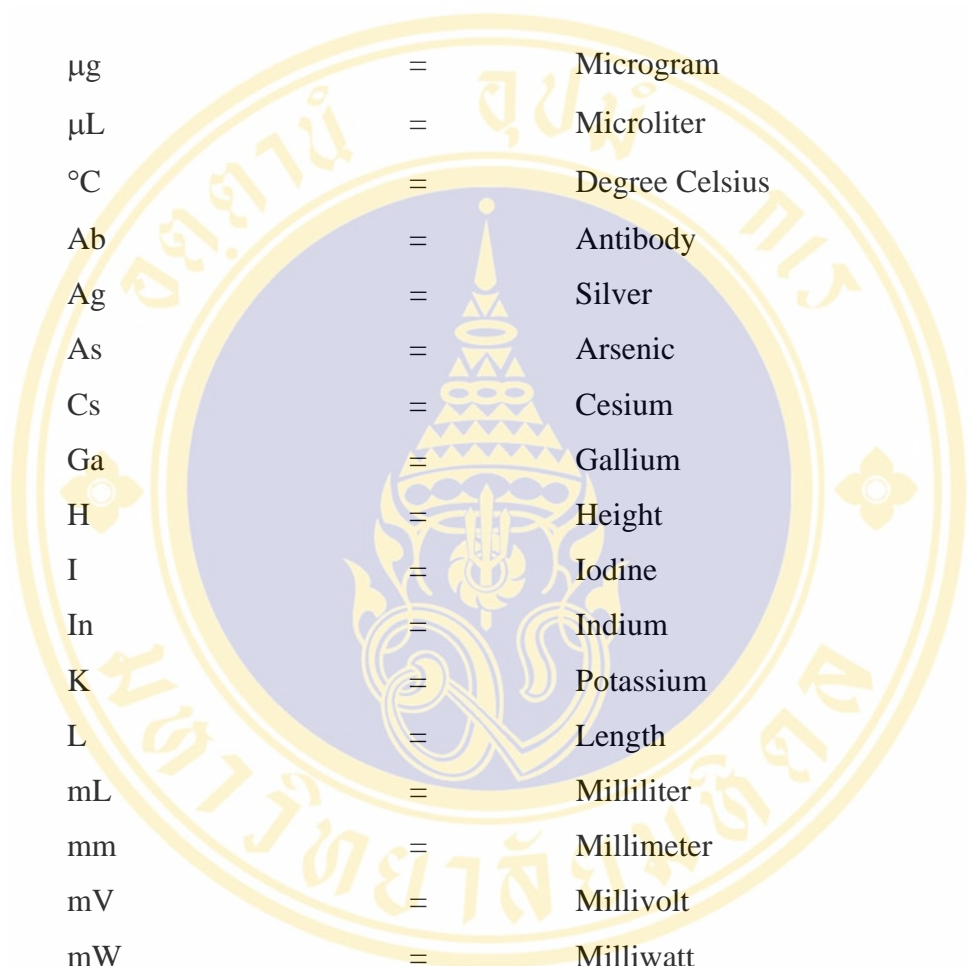
FIGURE	Page
2.1 Total internal reflection.	3
2.2 The exponentially decay of an evanescent wave at the surface of a different media.	4
2.3 The component of vector \vec{k}_2 in x-axis and z-axis.	6
2.4 The characteristic illustration of each term in eq. (10)	7
2.5 The simply illustration for fluorescent process.	9
2.6 The block diagram of Lock-in Amplifier.	10
2.7 The demodulator output of the signal in and reference signal with no phase shift.	10
2.8 The demodulator output of the signal in and reference signal with phase shift.	11
2.9 The cross-section schematic of head on type photomultiplier tube.	12
2.10 The external appearance of photomultiplier tube.	13
2.11 Types of Photocathode.	14
2.12 The structure of circular-cage type.	15
2.13 The structure of box-and-grid type.	15
2.14 The structure of linear-focused type.	15
2.15 The structure of venetian blind type.	16
2.16 The structure of coarse and fine mesh type.	16
2.17 The structure of microchannel plate.	17
2.18 The structure of metal channel type.	17
2.19 Elements of a laser.	20
2.20 The disposable coupon.	25
2.21 The illustrator of system set up in USA patent 4,909,990.	26
2.22 The planar waveguide in USA patent 6,611,634.	27
2.23 The system set up in USA patent 6,611,634.	28
3.1 The illustration of sensor chip design.	30

LIST OF FIGURES

(continued)

FIGURE	Page
3.2 The simple block diagram of the system set up.	33
3.3 The immobilized area on the cover plate.	34
4.1 The decayed wave at different θ_i .	36
4.2 The spectrum of laser source and the spectrum of fluorescent emission.	38
4.3 The comparison between the spectrum obtained from spectrophotometer (A) and the spectrum given from the manufacturer (B) [27].	38
4.4 The intensity of the fluorescent emission obtained from photomultiplier tube.	40
4.5 Response of fluorescent signal to the different concentration of Cyanine 5 at various measuring time.	42
4.6 Correlation between concentration of Cyanine 5 and fluorescent signal obtained from system set up.	43
4.7 The signal acquired from immobilized sensor chip.	45
4.8 The comparison of the signal acquired from three difference sensor chip.	47
4.9 The signal of the Cyanine 5 labeled albumin immobilized on cover plate.	49
4.10 The driver circuit of the laser diode.	50
4.11 The cross-section illustrator of optical module.	51
4.12 The block diagram of the developed system set up.	51
4.13 The illustrator of developed sensor chip.	52
4.14 The signals of dilution of Cyanine 5 labeled albumin.	54
4.15 Correlation between concentration of Cyanine 5 labeled albumin and fluorescent signal obtained from developed system.	55

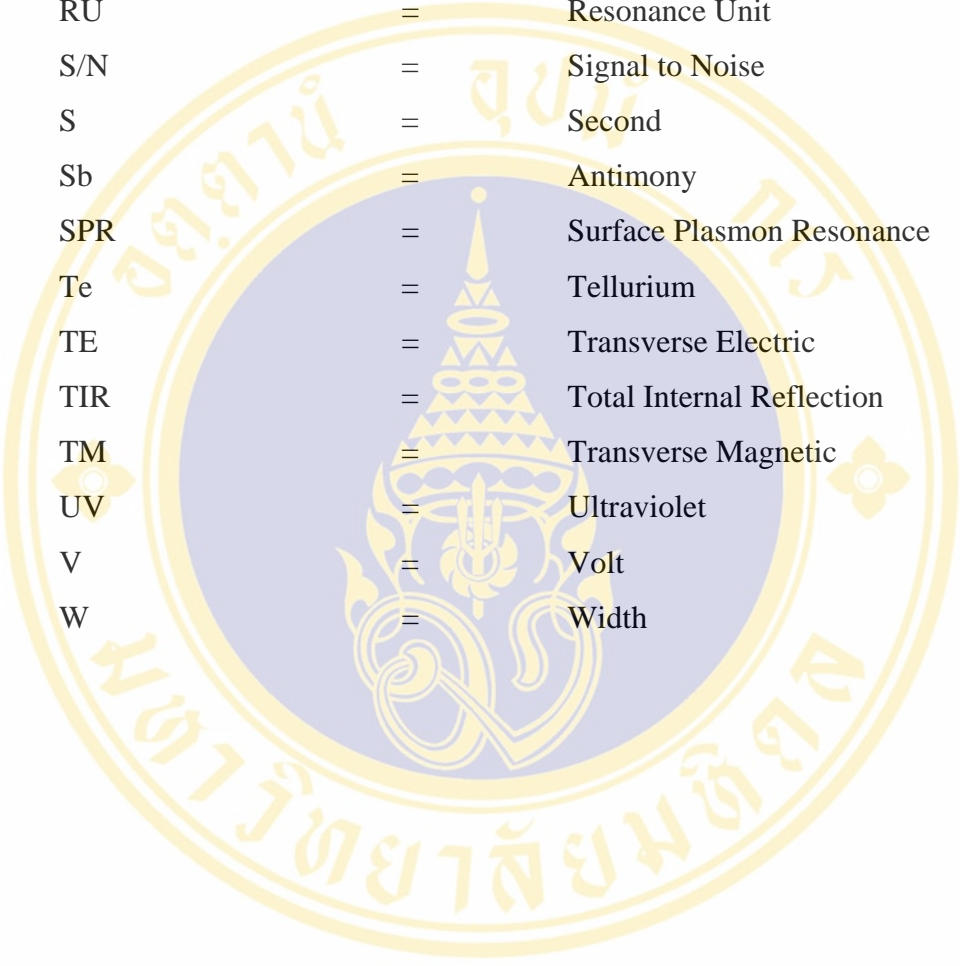
LIST OF ABBREVIATIONS



μg	=	Microgram
μL	=	Microliter
$^{\circ}\text{C}$	=	Degree Celsius
Ab	=	Antibody
Ag	=	Silver
As	=	Arsenic
Cs	=	Cesium
Ga	=	Gallium
H	=	Height
I	=	Iodine
In	=	Indium
K	=	Potassium
L	=	Length
mL	=	Milliliter
mm	=	Millimeter
mV	=	Millivolt
mW	=	Milliwatt
Na	=	Sodium
nm	=	Nanometer
O	=	Oxygen
OWLS	=	Optical Waveguide Lightmode Spectroscopy
PBS	=	Phosphate Buffer Saline
PCB	=	Printed Circuit Board
PMMA	=	Polymethyl Methacrylate
PMT	=	Photomultiplier Tube
PSD	=	Phase-Sensitive Detector

LIST OF ABBREVIATIONS

(continued)



Rb	=	Rubidium
RU	=	Resonance Unit
S/N	=	Signal to Noise
S	=	Second
Sb	=	Antimony
SPR	=	Surface Plasmon Resonance
Te	=	Tellurium
TE	=	Transverse Electric
TIR	=	Total Internal Reflection
TM	=	Transverse Magnetic
UV	=	Ultraviolet
V	=	Volt
W	=	Width

CHAPTER I

INTRODUCTION

1.1 Background

The technology for the biosensing has rapidly been developed owing to the progress in the telecommunication field. The term of optical detection for detecting the biocomponent has been brought into the biomedical science. The commonly known in optical application in biomedical science is the spectrometer, which utilize the properties of the absorbance and transmittance of light in different solutions for acquiring the concentration of the sample to be measured. In addition, there are other applications of the optical technique to be applied in biomedical science.

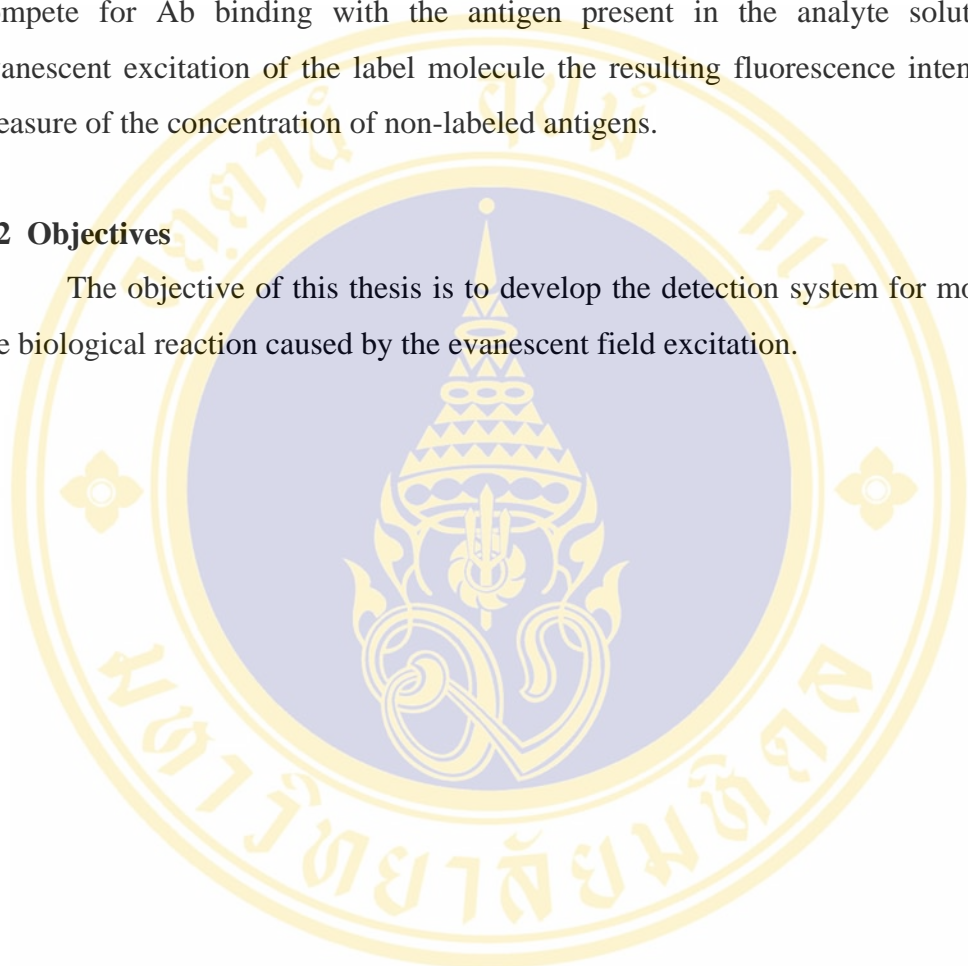
The fluorescence immunoassay is one of the techniques that utilize the optical theory for analyzing the clinical specimen. Fluorescence immunoassays or fluorescence immunosensors have already been generally used for a long time. They serve mainly in a liquid sample matrix, to quantify an unknown amount of a specific chemical or biochemical substance [1]. Normally, immunosensors take the advantage of the antigen-antibody reaction along with the use of the fluorophore to quantify the concentration of the sample. In those applications, the fluorophore will not be excited by the direct light but will be excited by the electromagnetic field called evanescent wave.

The evanescent wave is a well known physical phenomenon used in several types of chemo-optical sensors such as grating couplers, surface plasmon resonance sensors and optical fiber fluorescence sensors [2, 3, 4, 5]. It occurs on total internal reflection of plane waves at the interface of two mediums. The relatively short penetration depth of the evanescent wave makes it very suitable for measuring optical changes at this interface. This advantage of the evanescent wave is called “surface specific determination”. Additional specific advantages of a optical fiber fluorescence sensor are the long interaction length and the high efficiency for collection of fluorescence emitted near the core of the fiber [6].

In an evanescent fluorescence immunosensor, an antibody (Ab), immobilized onto the wave-guide surface, is used as a selector molecule to detect quantitatively and specifically the presence of an antigen in the sample to be analysed. This is accomplished by adding a known amount of fluorescently labeled antigen, which will compete for Ab binding with the antigen present in the analyte solution. On evanescent excitation of the label molecule the resulting fluorescence intensity is a measure of the concentration of non-labeled antigens.

1.2 Objectives

The objective of this thesis is to develop the detection system for monitoring the biological reaction caused by the evanescent field excitation.



CHAPTER II

LITERATURE REVIEW

In this chapter the theory of evanescent fluorescence and working theory of components are described.

2.1 Theory

2.1.1 Total internal reflection and evanescent wave

The basic principle of an optic fiber is total internal reflection. The total internal reflection is described by Snell's law and can be depicted as figure 2.1.

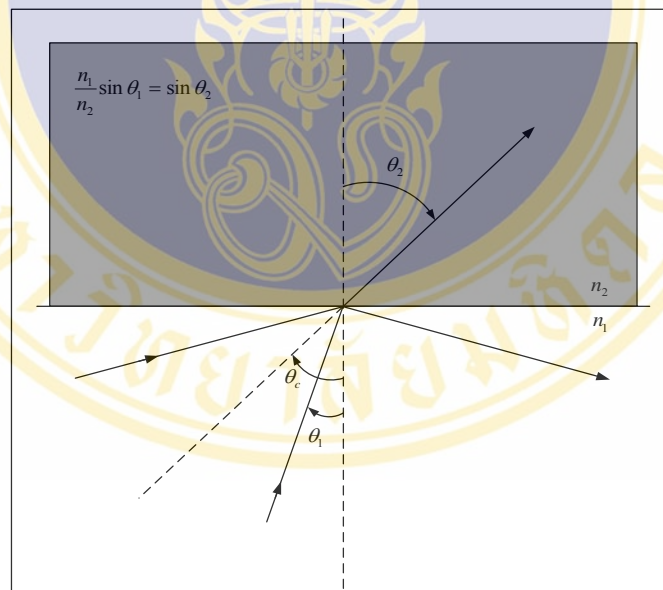


Figure 2.1 Total internal reflection.

A ray of light striking nearly perpendicular to the interface of two media with difference refractive index is refracted in a manner described by Snell's law. At an angle closer to the horizontal, the incident beam is no longer refracted into second medium, but is totally internally reflected at the interface. The critical angle which

defined the onset of total internal reflection can be determined from the refractive index of two media.

However, this simple Snell's law description fails to account for the several phenomena important in optical biosensor. Perhaps most important of these is so-called evanescent wave. In figure 2.1, when the incident light is totally internally reflected, the intensity does not abruptly fall to zero at the interface. Rather, the electromagnetic field intensity decays exponentially with distance starting from the interface and extending into the medium of lower refractive index [7]. The electromagnetic field component close to the interface is called the evanescent wave and is characterized by the penetration depth. The evanescent electromagnetic field, so-called evanescent wave, can interact with molecules in the surrounding medium near the interface, thereby producing absorption and fluorescent with incident light of the appropriate wavelength. The exponentially decay of an evanescent wave can be illustrated as figure 2.2.

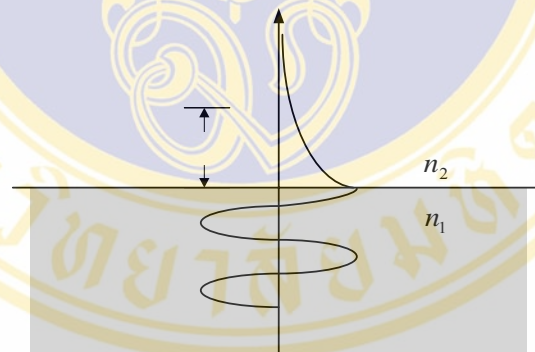


Figure 2.2 The exponentially decay of an evanescent wave at the surface of a different media.

According to figure 2.2, to demonstrate the range of penetration depth of evanescent wave propagates from the interface of the first medium n_1 , high refractive index, to second medium of low refractive index, n_2 , the penetration depth can be obtained from the principle of Snell's law. From Snell's law [8],

$$n_1 \sin \theta_1 = n_2 \sin \theta_2 \quad (1)$$

Eq. (1) can be rewritten to

$$\sin \theta_1 = \frac{n_2}{n_1} \sin \theta_2 \quad (2)$$

According to TIR's theory, TIR will be occur only when $n_1 > n_2$ and $\theta_1 > \theta_c$. So,

$$\sin \theta_1 = \sin \theta_c = \frac{n_2}{n_1} \sin \theta_2 \quad (3)$$

At critical angle, $\theta_2 = 90^\circ$. Thus, eq. (3) can be reduces to

$$\theta_c = \sin^{-1} \frac{n_2}{n_1} \quad (4)$$

Beyond the critical angle θ_c , the value of angle θ_2 becomes imaginary. To understand how the angle becomes imaginary, recall that [8]

$$\cos \theta_2 = \sqrt{1 - \sin^2 \theta_2}$$

By substituting, $\sin \theta_2 = \frac{n_1}{n_2} \sin \theta_1$, thus

$$\cos \theta_2 = \sqrt{1 - \left(\frac{n_1}{n_2}\right)^2 \sin^2 \theta_1} = \sqrt{1 - \frac{\sin^2 \theta_1}{\sin^2 \theta_c}}$$

In case of TIR, $\theta_1 > \theta_c$, the result of $\sin^2 \theta_1 / \sin^2 \theta_c > 1$.

So, $\cos \theta_2$ becomes imaginary.

$$\cos \theta_2 = \sqrt{1 + i^2 \frac{\sin^2 \theta_1}{\sin^2 \theta_c}} = i \sqrt{\frac{\sin^2 \theta_1}{\sin^2 \theta_c} - 1} \quad (5)$$

Considering electromagnetic wave, the electric field of wave can be written in term of \vec{k} - wave vector as

$$\vec{E} = \vec{E}_0 e^{i\vec{k}\cdot\vec{r}} e^{i\omega t} \quad (6)$$

where,

\vec{E}_0 = Amplitude

\vec{r} = Position vector

$e^{i\vec{k}\cdot\vec{r}}$ = Propagation term

$e^{i\omega t}$ = Time – dependent term

$$\vec{k} \propto \frac{2\pi}{n\lambda_0}$$

Consider only distance-related term,

$$e^{i\vec{k}\cdot\vec{r}} = e^{i(k_x X + k_y Y + k_z Z)} \tag{7}$$

According to figure 2-3, the transmitted wave propagates parallel to the xz plane.

Thus, $k_y = 0$.

$$e^{i\vec{k}\cdot\vec{r}} = e^{i(k_x X + k_z Z)} \tag{8}$$

the vector \vec{k} in medium 2 can be divided in to two components, in x-axis and z- axis, as shown in figure 2-3.

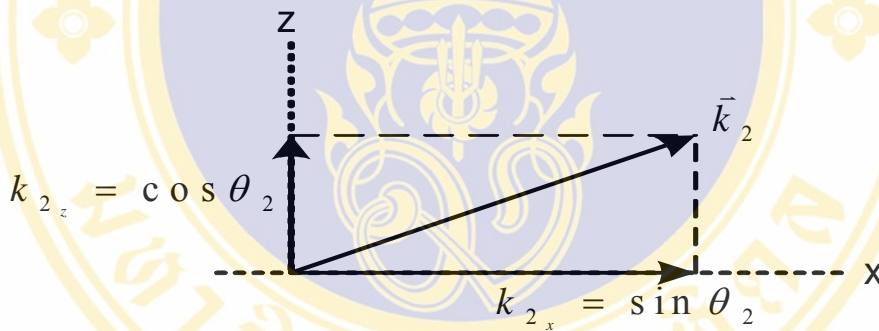


Figure 2.3 The component of vector \vec{k}_2 in x-axis and z-axis.

Thus,

$$e^{i\vec{k}_2\cdot\vec{r}} = e^{i(k_2 X \sin \theta_2 + k_2 Z \cos \theta_2)} \tag{9}$$

From eq. (2) and (5), the eq. (9) becomes

$$\begin{aligned} e^{i\vec{k}_2\cdot\vec{r}} &= e^{i(k_2 X \frac{n_1}{n_2} \sin \theta_1 + k_2 Z i \sqrt{\frac{\sin^2 \theta_1}{\sin^2 \theta_c} - 1})} \\ &= e^{i k_2 X \frac{n_1}{n_2} \sin \theta_1} + e^{-k_2 Z \sqrt{\frac{\sin^2 \theta_1}{\sin^2 \theta_c} - 1}} \end{aligned} \tag{10}$$

According to eq. (10), the first term is a sinusoidal term and the second one is exponential term. The characteristic of each term can be illustrated as figure 2.4.

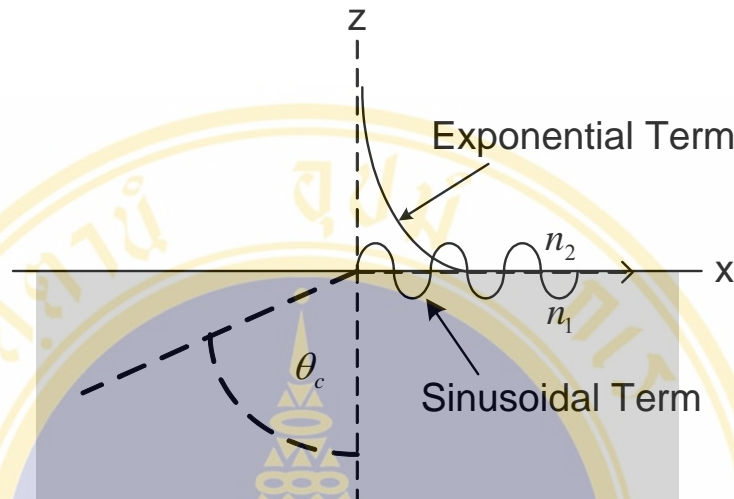


Figure 2.4 The characteristic illustration of each term in eq. (10).

As described above, the electric field of TIR in x-axis is a travelling wave. For z-axis, the electric field of TIR is a decayed wave and exponentially decays from the interface. Thus, the electric field in z-axis can be rewritten as:

$$I_{(z)} = I_{(z=0)} \exp\left(-\frac{z}{d}\right) \tag{11}$$

where d = penetration depth

From

$$I_{(z)} \propto |\vec{E}|^2 \propto |e^{i\vec{k}_2 \cdot \vec{r}}|^2 \propto \left(e^{-k_2 z \sqrt{\frac{\sin^2 \theta_1 - 1}{\sin^2 \theta_c}}} \right)^2$$

thus,

$$I_{(z)} = I_{(0)} e^{-2k_2 z \sqrt{\frac{\sin^2 \theta_1 - 1}{\sin^2 \theta_c}}}$$

$$I_{(z)} = I_{(0)} \exp\left(-\frac{z}{\frac{1}{2k \sqrt{\frac{\sin^2 \theta_1 - 1}{\sin^2 \theta_c}}}} \right) \tag{12}$$

comparing eq. (11) with eq. (12), therefore penetration depth is

$$\begin{aligned}
 d &= \frac{1}{2k \sqrt{\frac{\sin^2 \theta_1}{\sin^2 \theta_c} - 1}} & , k &= \frac{2\pi}{n_2 \lambda_0} \\
 &= \frac{\lambda_0}{4\pi \sqrt{\frac{1}{n_2^2} \frac{\sin^2 \theta_1}{\sin^2 \theta_c} - \frac{1}{n_2^2}}} & , \sin \theta_c &= \frac{n_2}{n_1} \\
 d &= \frac{\lambda_0}{4\pi \sqrt{n_1^2 \sin^2 \theta_i - n_2^2}} & , \theta_i &= \theta_1 \quad (13)
 \end{aligned}$$

2.1.2 Fluorescence [7, 9, 10]

One of the most sensitive techniques available to screen a small quantity out from the large numbers of target is the use of fluorescence. Fluorescence provides a unique sensitivity of light based system and combination of additional techniques. By definition, the fluorescence is the luminescence with the immediately energy released. The process of the fluorescence begins with molecule absorbs energy from photon of light and is excited to a higher electron state, excited state (S_2). When the molecule is in the excited state (S_2), it is undergoing changes such as conformational change and interacts with its environment in many different ways. All of these processes result in the absorbed energy in the excited state (S_2) is partially dissipated and molecule returns to intermediate state (S_1) where the fluorescent emission occurs. Then the molecule emits a photon of energy and returns back to ground state. It is important to note that not all of the excited species return to the ground state via fluorescent emission, many other processes can occur, such as fluorescence energy transfer, intersystem crossing or collisional quenching, which can remove molecules from S_1 . The simple illustrate for fluorescence process can be depicted in figure 2.5.

Another important property of fluorescence is that it occurs at a wavelength that is almost always longer than the absorbance (or excitation) wavelength. When photons due to a relaxation of molecules in an excited state are emitted, one of the most important observations is that they are emitted at longer wavelengths (lower frequency) and consequently are less energetic than the photons responsible for the excitation [9]. The difference between the excitation and emission is so called Stokes

shift. The Stokes shift represents the loss of energy whilst the molecule is in the excited state through energy transfer to environment before emission. The Stokes shift is important for many reasons but from a practical point of view it allows the emitted fluorescent photons to be easily distinguished from the excitation photons, leading to the possibility of very low backgrounds in fluorescent studies.

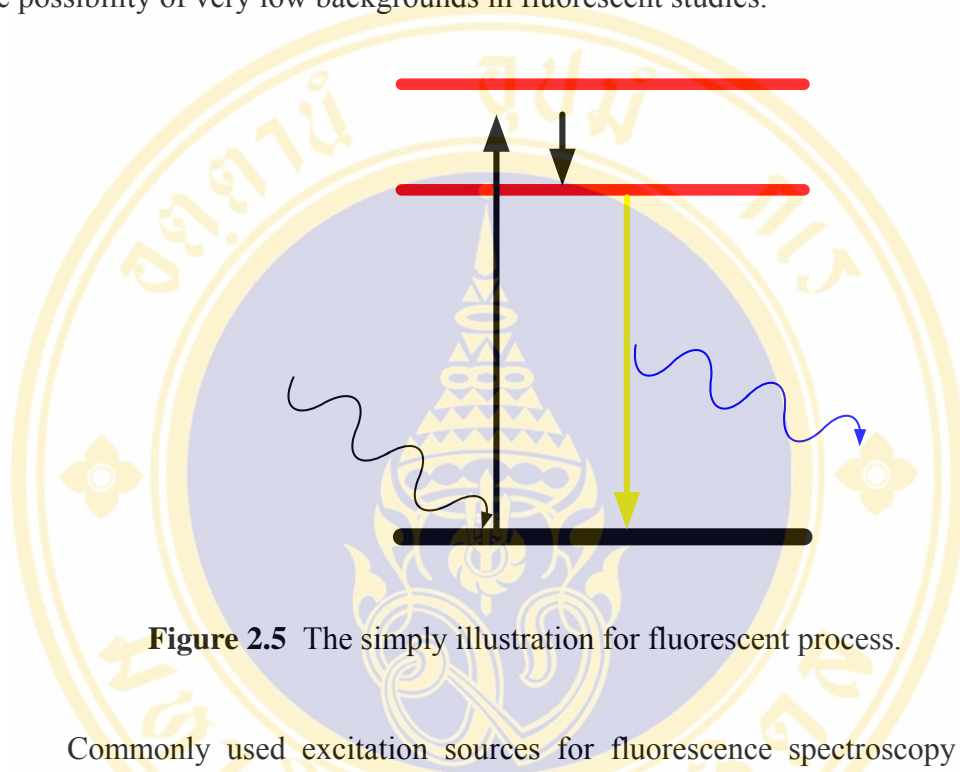


Figure 2.5 The simply illustration for fluorescent process.

Commonly used excitation sources for fluorescence spectroscopy includes tungsten, mercury arc, and xenon lamps. Each of these has both its characteristic intensity and its spectral output, which is not uniform with wavelength. Illumination that is commonly used for the high intensity or focused illumination that is required for the most sensitive detection of fluorescence. A major factor in the ultrasensitive measurement of fluorescence, especially in single-molecule detection, is the ability to focus on the extremely small volume of sample as in the case of flow cytometers and most laser scanning microscopy.

2.1.3 Lock-in Amplifier [11, 12]

Lock-in amplification is a technique that can be used to reduce noise and recover low level signal. The method involves modulating the signal by specific reference frequency and phase then detecting and amplifying the signal. Noise signals

at frequencies other than the reference frequency are rejected and do not affect the measurement. Block diagram of the lock-in amplifier can be illustrated as figure 2.6.

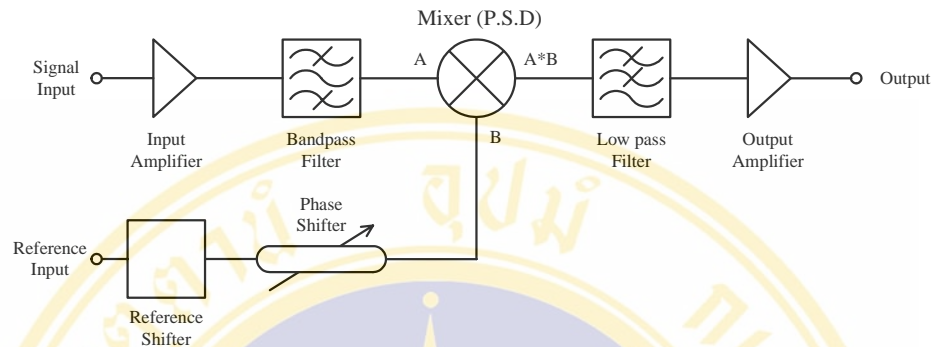


Figure 2.6 The block diagram of Lock-in Amplifier.

The heart of the lock-in amplifier is the phase-sensitive detector (PSD), which is also known as a demodulator or mixer. The detector operates by multiplying two signals together, and the analysis to provide the required outputs can be described as follow. Figure 2.7 shows the situation where the lock-in amplifier is detecting a noise-free sinusoid, identified in the diagram as “Signal In”. The instrument is also fed with a reference signal, which is also shown in the diagram.

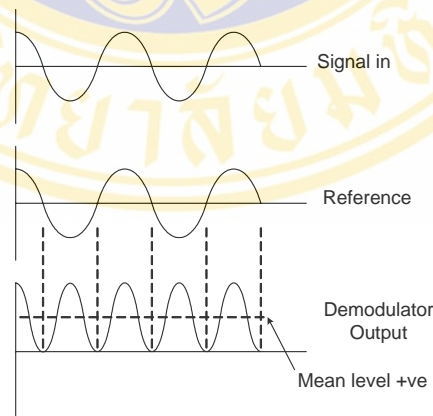


Figure 2.7 The demodulator output of the signal in and reference signal with no phase shift.

The demodulator operates by multiplying two signals together, resulting in the signal identified in the diagram as “Demodulator Output”. Since there is no relative

phase-shift between the signal and reference phases, the demodulator output takes the form of a sinusoid at twice of the reference frequency, but with a mean, or average, level which is positive. Figure 2.8 shows the same situation, except that the signal phase is now delayed by 90° with respect to the reference. It can be seen that although the output still contains a signal at twice the reference frequency, the mean level is now zero.

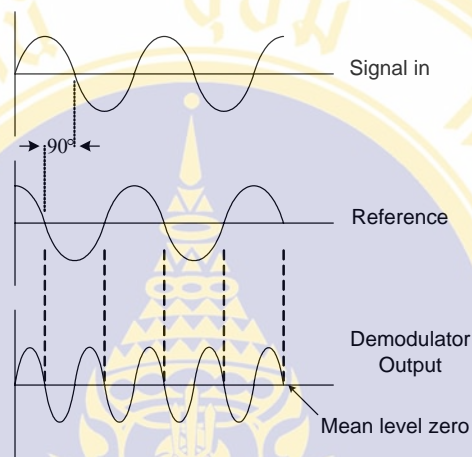


Figure 2.8 The demodulator output of the signal in and reference signal with phase shift.

From this it can be seen that the mean level is proportional to the product of the signal and reference frequency amplitudes, and related to the phase angle between the signal and reference.

The above discussion is based on the case of noise-free input signals, but in real applications the signal will be accompanied by noise. This noise, which by definition has no fixed frequency or phase relationship to the reference, is also multiplied by the reference signal in the demodulator, but does not result in any change to the mean DC level. Noise components at frequencies very close to that of the reference do result in demodulator outputs at very low frequencies, but by setting the low-pass filter to a sufficiently low cut-off frequency these can be rejected. Hence the combination of a demodulator and low-pass output filter allows signals to be measured even when accompanied by significant noise.

2.1.4 Photomultiplier Tube [13, 14]

The photomultiplier tube is a photon-sensitive device that converts the light energy to electrical energy and amplifies the resultant pulse of electricity. Among photosensitive devices in use today, the photomultiplier tube (PMT) is a versatile device providing ultra-fast response and extremely high sensitivity [14]. The photomultiplier tube consists of a photocathode followed by focusing electrodes, series of 10 or more dynodes (electron multiplier), and an electron collector (anode). An outer glass envelope provides a pressure boundary to sustain vacuum conditions inside the tube that are required so that low-energy electrons can be accelerated efficiently by internal electric fields. The simply structure of photomultiplier is shown in figure 2.9.

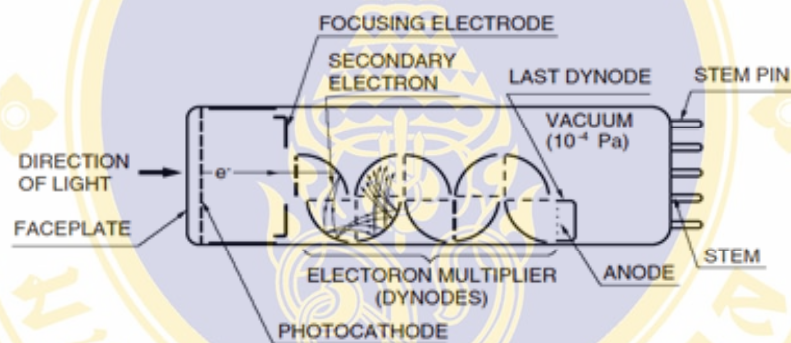


Figure 2.9 The cross-section schematic of head on type photomultiplier tube.

A brief process of amplification of photomultiplier can be described as follows. According to Figure 2.9, the photocathode receives the light wave from the source. The incident light wave hits the atoms of the photocathode and causes electrons to be ejected. This phenomena is called photoemission. The number of electron released is proportional to the intensity of the light from the source. Then, the electrons emitted from the photocathode directed by an electric field to first dynodes in the photomultiplier tube. This electric field is due to the applied voltage between the photocathode and that dynode. The electric field accelerates the electron with such force that when it strikes the dynode more than one electron is released from the dynode. This is called secondary emission. These electrons are then drawn to the

second dynode by a similar increase in applied voltage, whereas secondary emission takes place again. This process continues throughout the whole photomultiplier tube until a final gain. By the time the electrons have left the last dynode the number of electrons released may be on the order of millions. The photomultiplier tube therefore possesses the ability to convert one flash of light into millions of electrons.

Because of secondary-emission multiplication, photomultiplier tubes provide extremely high sensitivity and exceptionally low noise compared to other photosensitive devices currently used to detect radiant energy in the ultraviolet, visible, and near infrared regions. The photomultiplier tube also features fast time response and a choice of large photosensitive area. According to those advantages, the photomultiplier tube is widely used to detect a small signal.

2.1.4.1 Construction

The photomultiplier tube generally has a photocathode in either a side-on or a head-on configuration. The side-on type receives incident light through the side of the glass bulb, while the head-on type receives light through the end of the glass bulb. In general, the side-on type photomultiplier tube is relatively low priced and widely used for spectrophotometers and general photometric systems. Most side-on types employ an opaque photocathode (reflection-mode photocathode) and a circular-cage structure electron multiplier (detail was described in Electron Multiplier) which has good sensitivity and high amplification at a relatively low supply voltage.



Figure 2.10 The external appearance of photomultiplier tube.

The head-on type (or the end-on type) has a semitransparent photocathode (transmission-mode photocathode) deposited upon the inner surface of the entrance window. The head-on type provides better uniformity than the side-on type having a reflection-mode photocathode. Other features of head-on types include a choice of photosensitive areas ranging from tens to hundreds of square centimeters.

Variants of the head-on type having a large-diameter hemispherical window have been developed for high energy physics experiments where good angular light reception is important.

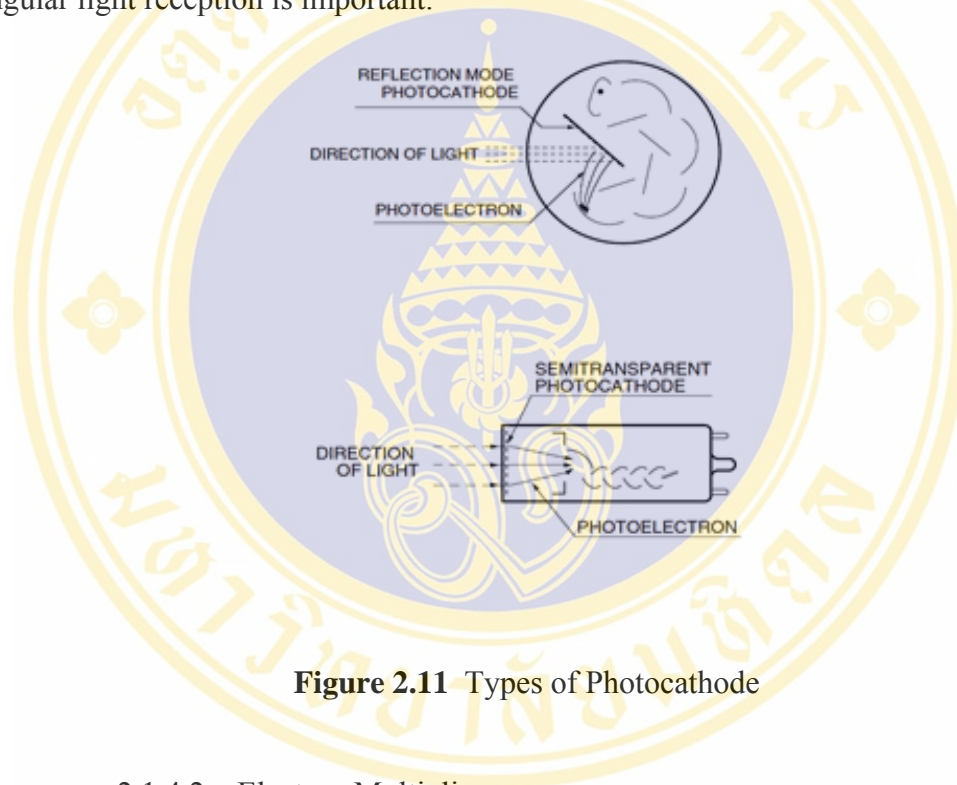


Figure 2.11 Types of Photocathode

2.1.4.2 Electron Multiplier

The superior sensitivity (high current amplification and high S/N ratio) of photomultiplier tubes is due to the use of a low-noise electron multiplier which amplifies electrons by a cascade secondary emission process. The electron multiplier consists of 8 to 19 stages of electrodes called dynodes. There are several principal types in use today.

1) Circular-cage type.

The circular cage is generally used for the side-on type of photomultiplier tube. The prime features of the circular-cage are

compactness, fast response and high gain obtained at a relatively low Supply voltage.



Figure 2.12 The structure of circular-cage type.

2) Box-and-grid type

This type consists of a train of quarter cylindrical dynodes and is widely used in head-on type photomultiplier tubes because of good electron collection efficiency and excellent uniformity.



Figure 2.13 The structure of box-and-grid type.

3) Linear-focused type

The linear-focused type features extremely fast response time and is widely used in applications where time resolution and pulse linearity are important. This type also has the advantage of providing a large output current.



Figure 2.14 The structure of linear-focused type.

4) Venetian blind type

The venetian blind type has a large dynode area and is primarily used for tubes with large photocathode areas. It offers better uniformity and a larger output current. This structure is usually used when time response is not a prime consideration.

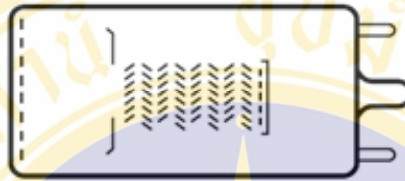


Figure 2.15 The structure of venetian blind type.

5) Mesh type

The mesh type has a structure of fine mesh electrodes stacked in close proximity. There are two mesh types of dynode. The first one is a coarse mesh type and the second one is a fine mesh type. Both types provide improved pulse linearity and high resistance to magnetic fields. The mesh type also has position-sensitive capability when used with cross-wire anodes or multiple anodes. The fine mesh type is particularly suited for use in applications where high magnetic fields are present.

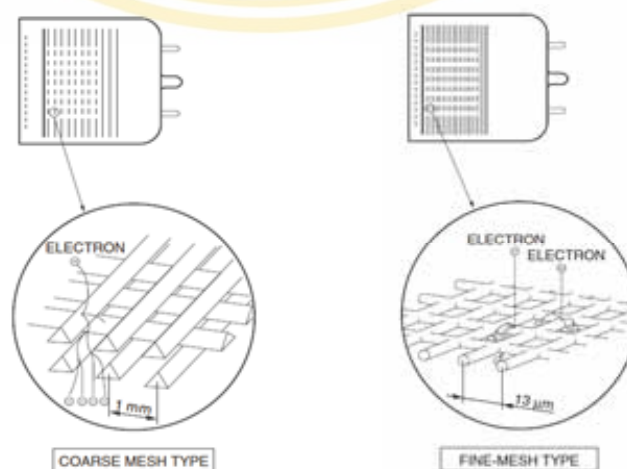


Figure 2.16 The structure of coarse and fine mesh type.

6) Microchannel plate (MCP)

The MCP is a thin disk consisting of millions of microglass tubes (channels) fused in parallel with each other. Each channel acts as an independent electron multiplier. The MCP offers much faster time response than other discrete dynodes. It also features good immunity from magnetic fields and two-dimensional detection ability when multiple anodes are used.



Figure 2.17 The structure of microchannel plate.

7) Metal Channel type

The metal channel dynode has a compact dynode construction manufactured by our unique fine machining techniques. It delivers high-speed response due to a space between each dynode stage that is much smaller than other types of conventional dynodes. The metal channel dynode is also ideal for position sensitive measurement.

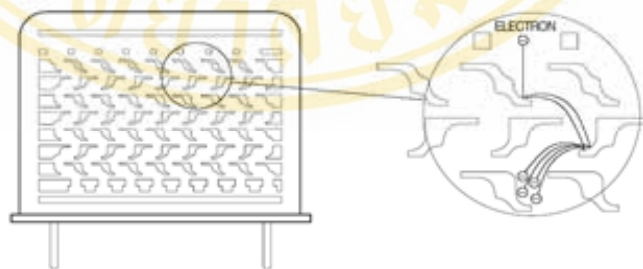


Figure 2.18 The structure of metal channel type.

Beside, there is other structure of electron multiplier called “Hybrid dynodes” which combining two of the above dynodes. These hybrid dynodes combine the best features of each dynode type.

2.1.4.3 Spectral response

The photocathode of a photomultiplier tube converts energy from incident light into electrons. The conversion efficiency (photocathode sensitivity) varies with the wavelength of the incident light. This relationship between photocathode sensitivity and wavelength is called the spectral response characteristic. The spectral response on long wavelengths is determined by the photocathode material and on short wavelengths by the window material.

2.1.4.4 Photocathode material

The photocathode consists of a material that responds to the waves of light energy, much like any atom responds to waves of gamma energy in the Compton Effect. The photocathode is a photoemissive surface, which usually consisting of alkali metals with very low work functions. The photocathode materials most commonly used in photomultiplier tubes are as follows:

1) Ag-O-Cs.

This material is response from the range of visible light to infrared radiation (300 nm to 1000 nm). The reflection mode covers a slightly narrower range from 300 nm to 1100 nm. Since Ag-O-Cs has comparatively high thermionic dark emission, photomultiplier tubes of this photocathode material are chiefly used for detection in the infrared region with the photocathode cooled.

2) GaAs.

GaAs activated in cesium is also used as a photocathode. The spectral response of this photocathode material usually covers a wider spectral response range than multialkali, from ultraviolet to 930 nm, which is comparatively flat over the range between 300 nm and 850 nm.

3) InGaAs.

This photocathode material has greater extended sensitivity in the infrared range than GaAs. Moreover, in the range between 900 nm and 1000 nm, InGaAs has a much higher S/N ratio than Ag-O-Cs. Some photocathodes can operate at 1700 nm.

4) Sb-Cs.

Sb-Cs has a spectral response in the ultraviolet to visible range and is mainly used in reflection-mode photocathodes.

5) Bialkali (Sb-Rb-Cs, Sb-K-Cs).

These materials have a spectral response range similar to the Sb-Cs photocathode, but have higher sensitivity and lower dark current than Sb-Cs. They also have a blue sensitivity index matching the scintillation flashes of NaI scintillators and so are frequently used for radiation measurement using scintillation counting.

6) High temperature bialkali or low noise bialkali (Na-K-Sb).

This is particularly useful at higher operating temperatures since it can withstand up to 175 °C. At room temperatures, this photocathode operates with very low dark current, making it ideal for use in photon counting applications.

7) Multialkali (Na-K-Sb-Cs).

The multialkali photocathode has a high, wide spectral response from the ultraviolet to near infrared region. It is widely used for broad-band spectrophotometers and photon counting applications. The long wavelength response can be extended to 930 nm by a special photocathode activation processing.

8) Cs-Te, Cs-I.

These materials are sensitive to vacuum UV and UV rays but not to visible light and are therefore referred to as solar blind. Cs-Te is quite insensitive to wavelengths longer than 320 nm, and Cs-I to those longer than 200 nm.

2.1.5 Laser source [15, 16 17]

Laser is an acronym for 'Light Amplification of Stimulated Emission of Radiation'. A laser is a device that controls the way that energized atoms release photons. It creates and amplifies a narrow, intense beam of coherent light. Laser consists of four necessary elements to produce coherent light by stimulated emission of radiation. These four function elements are illustrated in figure 2.19.

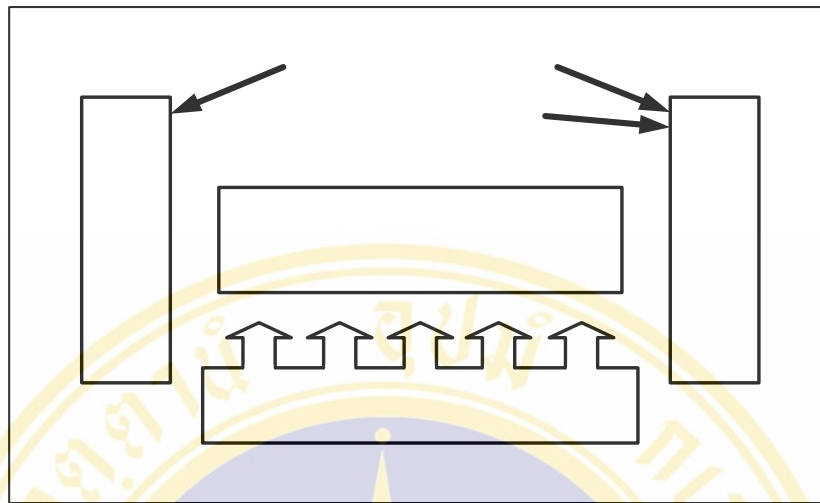


Figure 2.19 Elements of a laser

2.1.5.1 The element of laser

As shown in figure 2.19, laser consists of four important elements to produce a laser beam.

1) Active medium.

The active medium is a collection of atoms or molecules that can be excited to a state of inverted population where more atoms or molecules are in an excited state than in some lower energy state. The active medium may be a gas, a liquid, a solid material, or a junction between two slabs of semiconductor materials. The two states chosen for the lasing transition must possess certain characteristics. First, atoms must remain in the upper lasing level for a relatively long time to provide more emitted photons by stimulated emission than by spontaneous emission. Second, there must be an effective method of "pumping" atoms from the highly-populated ground state into the upper lasing state in order to increase the population of the higher energy level over the population in the lower energy level. An increase in population of the lower energy level to a number above that in the high energy level will negate the population inversion and thereby prevent the amplifications of emitted light by stimulated emission.

The active medium of a laser can be thought of as an optical amplifier. A beam of coherent light entering one end of the active medium is amplified through

stimulated emission until a coherent beam of increased intensity leaves the other end of the active medium. Thus, the active medium provides optical gain in the laser.

2) Excitation mechanism

The excitation mechanism is a source of energy that excites, or "pumps," the atoms in the active medium from a lower to a higher energy state in order to create a population inversion. In gas lasers and semiconductor lasers, the excitation mechanism usually consists of an electrical-current flow through the active medium. Most of solid and liquid lasers often employ optical pumps; for example, in a ruby laser, the chromium atoms inside the ruby crystal may be pumped into an excited state by means of a powerful burst of light from a flashlamp containing xenon gas.

3) Feedback mechanism

The feedback mechanism returns a portion of the coherent light originally produced in the active medium back to the active medium for further amplification by stimulated emission. The amount of coherent light produced by stimulated emission depends upon both the degree of population inversion and the strength of the stimulating signal. The feedback mechanism usually consists of two mirrors, one at each end of the active medium, aligned in such a manner that they reflect the coherent light back and forth through the active medium.

4) Output Coupler

The output coupler allows a portion of the laser light contained between the two mirrors to leave the laser in the form of a beam. One of the mirrors of the feedback mechanism allows some light to be transmitted through it at the laser wavelength. The fraction of the coherent light allowed to escape varies greatly from one laser to another--from less than one percent for some helium-neon lasers to more than 80 percent for many solid-state lasers.

2.1.5.2 Lasing process

For the lasing process, when the excitation mechanism of a laser is activated, energy flows into the active medium, causing atoms to move from the ground state to certain excited states. In this way, population inversion is created. Some of the atoms in the upper lasing level drop to the lower lasing level

spontaneously, emitting incoherent photons at the laser wavelength and in random directions. Most of these photons escape from the active medium, but those that travel along the axis of the active medium produce stimulated emission. The beam produced is reflected back through the active medium by the mirrors. A portion of the light that strikes the output coupler leaves the laser as the output beam.

2.1.5.3 Type of laser

There are many different types of lasers. Lasers may be classified according to the type of active medium, excitation mechanism, or duration of laser output. Classification by active medium is utilized here.

The laser medium can be a solid, gas, liquid or semiconductor. Lasers are commonly designated by the type of lasing material employed:

1) Solid-state laser

Solid-state lasers have lasing material distributed in a solid matrix (such as the ruby or neodymium:yttrium-aluminum garnet "Yag" lasers). The neodymium-Yag laser emits infrared light at 1,064 nanometers (nm). A nanometer is 1×10^{-9} meters.

2) Gas laser

Gas lasers have a primary output of visible red light. Helium and helium-neon, HeNe, are the most common gas lasers. CO₂ lasers emit energy in the far-infrared, and are used for cutting hard materials.

3) Excimer laser

Excimer lasers use reactive gases, such as chlorine and fluorine, mixed with inert gases such as argon, krypton or xenon. When electrically stimulated, a pseudo molecule (dimer) is produced. When lased, the dimer produces light in the ultraviolet range.

4) Dye laser

Dye lasers use complex organic dyes, such as rhodamine 6G, in liquid solution or suspension as lasing media. They are tunable over a broad range of wavelengths.

5) Semiconductor laser

Semiconductor lasers, sometimes called diode lasers, are not solid-state lasers. These electronic devices are generally very small and use low power. They may be built into larger arrays, such as the writing source in some laser printers or CD players.

2.2 Related work

The advantage of evanescent wave was used along with the other techniques to performed many type of biosensor, such as:

2.2.1 Surface plasmon resonance (SPR) [7, 18, 19]

The SPR system utilized the evanescent wave technique to excite the surface plasmons in metal film. The general principle of SPR measurement begins with the polarized light propagates from a layer of high refractive index towards a layer with low refractive index resulting in total internal reflection. The sample is attached to the layer of low refractive index. At the interface between the two different media, a thin approximately 50 nm gold film is interposed. Although light totally internally reflects back to the high refractive index medium, the intensity does not equal to zero at the interface, as described in theory in total internal reflection. Physical requirements of continuity across the interface are the cause of excitation of surface plasmons in the metal film by the light energy, causing them to oscillate. This produces an exponential evanescent decaying, which penetrates a defined distance into the low-index medium and results in a characteristic decrease in reflected light intensity. By monitoring the intensity and the resonance angle of the reflected light, the changes of the refractive index at the surface interface causes by the biospecific interactions are detected.

For example, BIAcore (Pharmacia Biosensor), a well known commercial biosensor, is based on surface plasmon resonance (SPR) for detection of changes in refractive index at the sensory surface. These changes are proportional to the mass of molecules bound to the surface, and are shown in a 'sensorgram' as resonance units (RU) plotted against time. From the results, stoichiometric and kinetic data for the interaction can be determined.

In Wood's work [20], a reaction surface was prepared in BIAcore by covalent coupling of a ligand to the derivatized dextran matrix located on a sensor chip surface.

Four areas of the chip surface were used as unique reaction chambers. Each chamber was individually fed by a fluid channel. Although primary ligands were bound to the dextran matrix, reaction proceeded in a liquid environment. Microliter amounts of reactants were delivered by operator-programmed software. Reaction surfaces, bound to a 50-nm gold surface, were mechanically brought in contact with the glass interface of the optical system. Monochromatic light, deflected at the reaction surface, was reflected as a function of the difference in refractive indices of the glass and liquid layer. A part of the resulting total internal reflectance of light was monitored as the reaction occurred. Concomitant to reflectance, evanescent wave energy was generated within the metal surface. This change was monitored electronically using a separate diode array for each of the four channels and recorded graphically as reactions occurred. The hybridization reaction was carried out at room temperature and positive signals were obtained within 7 minutes. This was the first account of real-time detection of specific hybridization within a fluid flow system in less than 10 minutes at room temperature [20].

2.2.2 Total internal reflection fluorescence

The total internal reflection fluorescence utilizes benefit from phenomenon of evanescent wave along with the characteristic of fluorophore. The process of total internal reflection fluorescence starts in the same way to the surface plasmon resonance. The total internal reflection produces an evanescent wave at the interface of two mediums. The intensity of electromagnetic field, evanescent wave, decays exponentially with distance starting from the interface and extending into the low-index medium. As a result, the fluorophores in range of evanescent wave are excited and emitted fluorescence.

The total internal reflection fluorescence system can be classified according to the shape of the waveguide of optical probe which are fiberoptic waveguide and planar waveguide.

For example of the fiberoptic waveguide, RAPTOR is the one commercial optical biosensor that used this technique. The RAPTOR is a portable automated fiber optic biosensor for detection of biological threat agents. It performs rapid, fluorescent sandwich immunoassays on the optical probe for up to four target analytes

simultaneously [21]. The optical probe can be reused up to forty times or until positive result is obtained. The RAPTOR is useful for on-site analysis of food, water, or clinical samples for biological contaminants [21, 22].

The system employs a separate 635 nm laser diode to excite each of the four fiber optic probes. In order to match the excitation wavelength, the fluorescent dye Cyanine 5 is used to tag the tracer antibody. The polystyrene is used to provide a fiber optic probe by inject-molded. The fiber optic probes are blackended at their distal end to prevent reflection of excitation light. The capture antibodies are immobilized onto the fiber optic probes by passive adsorption. After capture antibodies immobilization and pre-treat process, the optical fiber probe then mounted and glued into the disposable coupons. The illustration of disposable coupon is depicted as figure 2.20.

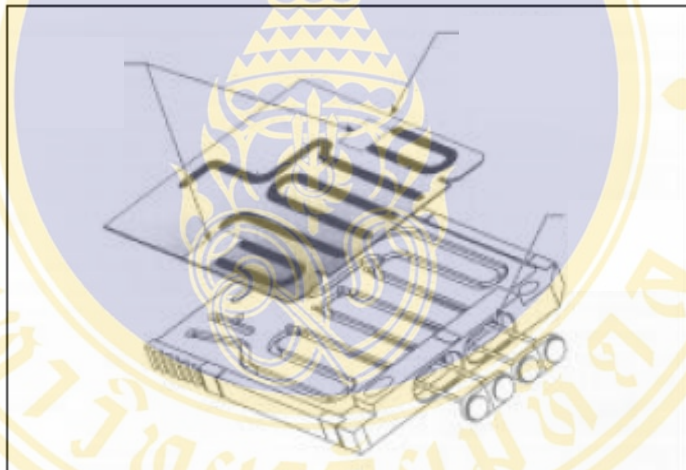


Figure 2.20 The disposable coupon.

For the operation, the assay coupon is inserted into the RAPTOR coupon compartment. The excitation laser is focused into the fiber optic probe. The evanescent wave causing by excitation laser is created along each probes. The portion of evanescent fluorescent emission captured by optical probe is collimated by molded ball lens at the head of the probe and focus onto a photodiode.

For more examples, in USA Patent 4,909,990[23], the optical rod (fiber) is used as a waveguide. A component of a complex formed in an immunochemical reaction is immobilized on the optical rod. A fluorophore is attached to another

component of the complex. The fluorescent labeled component may be either the complement to or the analog of the immobilized component, depending upon whether competitive or sandwich assays are to be performed. The length of the optical rod is equal to 4 centimeters and its diameter is equal to 1 millimeter. The optical rod is aligned to the system by the fiber centering device which comprises fixed spring mount, slidable spider and tension spring. The fiber and the attached constituent of the assay are immersed in a fluid phase sample.

The excitation beam generated from the light source is folded by beam splitter and pass through objective lens into an input end of rod and totally internally reflects along optical rod. Multiple total internal reflections in the optical rod allow the excitation beam to excite repeatedly an evanescent wave. The evanescent wave is used to excite fluorescence in the fluid phase. All of the radiation fluorescence that tunnels back into the fiber within the total reflection angle is thus trapped within the fiber and detected at the input end of the fiber by photo detector. The illustration of system set up can be depicted as figure 2.21.

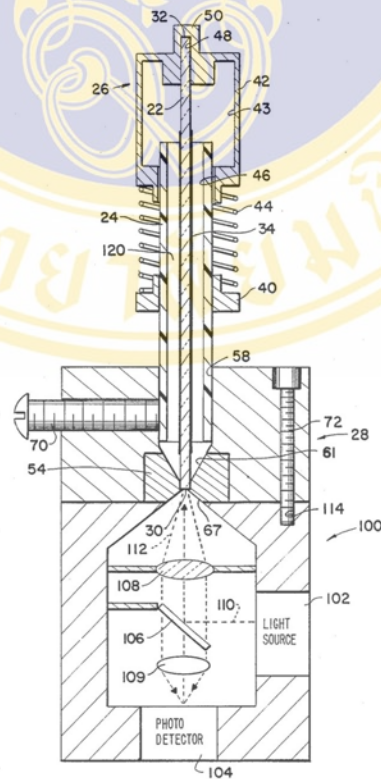


Figure 2.21 The illustration of system set up in USA patent 4,909,990.

For the example of system set up which employed a planar waveguide, USA patent 6,611,634 B2 [24], an optical biosensor with reservoirs is described. The illustrator of planar waveguide is shown in figure 2.22. The plastic molded plate with an integrated input (see 166 in figure 2.22) and output (see 168 in figure 2.22) coupling lenses is used as a waveguide. The capture antibody is immobilized on the surface of the waveguide. At the top of the waveguide, a flow cell which made from light-absorbing material is placed. The flow cell is also functioned as a wall of reservoir. Between the waveguide and the flow cell, the Teflon gasket is placed to prevent a leakage of the sample. The excitation beam is directed by means of mirrors as shown in figure 2.23 before is introduced into the coupling lens at the front end of waveguide. The excitation internally propagates inside a waveguide to produce an evanescent wave. Fluorescence-emitting tracer molecules are bound to the waveguide surface. The emitted fluorescence is directly collected by a collection lens then sent to the light detection which responds by outputting signals reflective of the level of collected fluorescence.

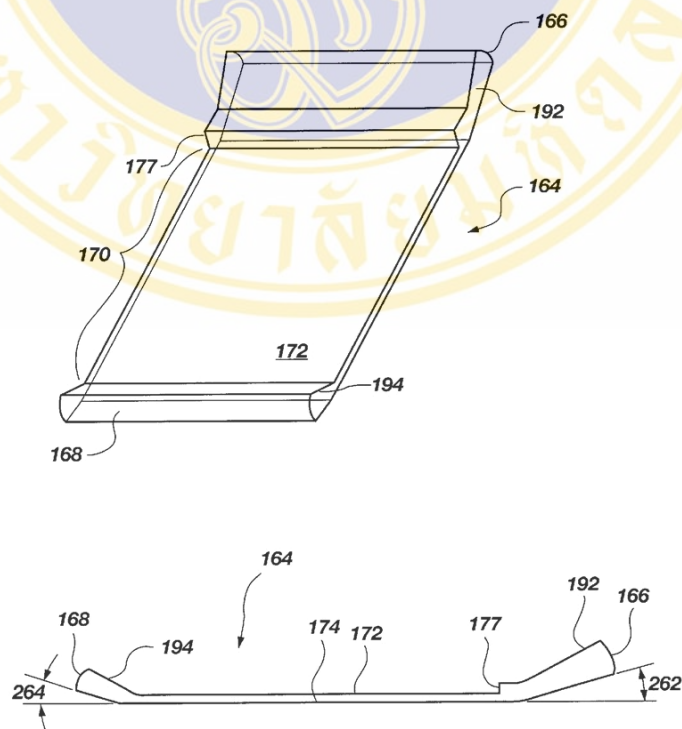


Figure 2.22 The planar waveguide in USA patent 6,611,634.

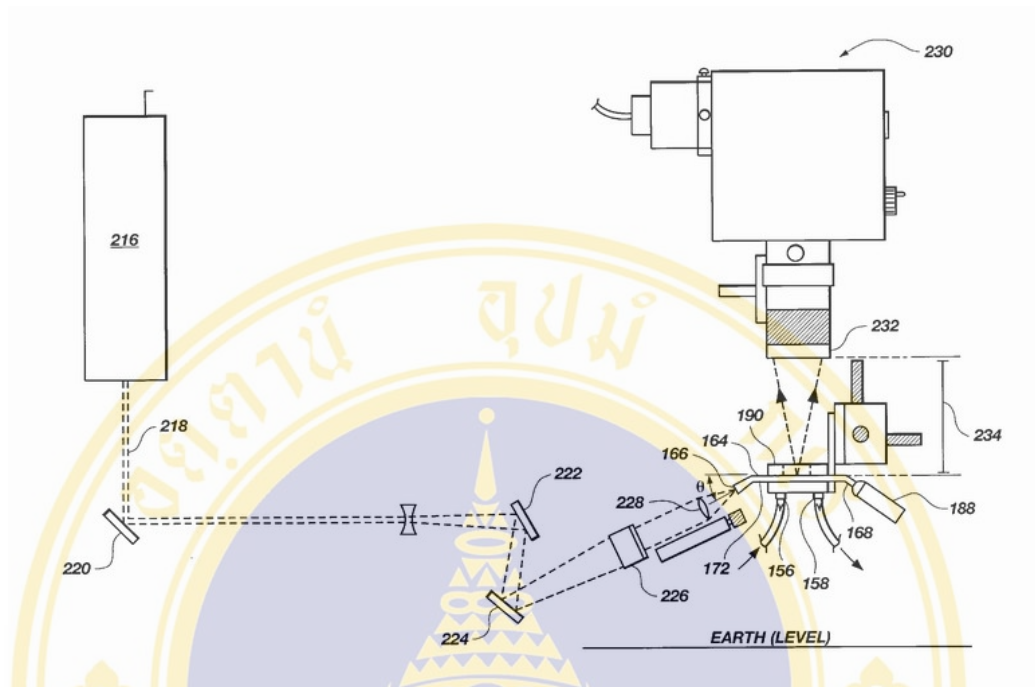


Figure 2.23 The system set up in USA patent 6,611,634.

2.2.3 Grating coupler

Grating coupler is a device used to measure the coupling angle of either the input or output laser beam. Both beams are correlated to the refractive index within the evanescent field at the sensor's surface. Grating couplers are also used for optical waveguide lightmode spectroscopy (OWLS) [25, 26]. The basic principle of the OWLS method is that linearly polarized light is coupled by a diffraction grating into the waveguide layer. The incoupling is a resonance phenomenon that occurs at a defined angle of incidence that depends on the refractive index of the medium covering the surface of the waveguide. In the waveguide layer, light is guided by total internal reflection to the edges where it is detected by photodiodes. By varying the angle of incidence of the light, the mode spectrum is obtained from which the effective refractive indexes are calculated for both TE and TM.

CHAPTER III

MATERIALS AND METHODS

3.1 Materials

3.1.1 Chemicals

A Cyanine 5TM, the fluorescence dye model PA 25001 was purchased from the Amercham life science, Inc. A bovine serum albumin and other common chemicals were obtained from Sigma, USA.

3.1.2 Optical equipments

For system set up, the laser diode from the Lasermx, Inc. and Thorlabs, Inc. were used as a light source for the primary and the developed set up respectively. The laser diode model LSX 635-5C from Lasermx, Inc. has 4.25 mW maximum output power with wavelength of 635 nanometers. For model HL6312G from Thorlabs, Inc., the laser diode has 5mW maximum output power with the same wavelength with LSX 635-5C. All optical lenses were purchased from Thorlabs, Inc. Various focus length of 1 inch diameter plano – convex lenses were used to collected and collimated. A one inch diameter interference filter with a wavelength of 670 nanometers was also obtained from Thorlabs, Inc.

3.1.3 Sensor chip and design

The sensor chip consists of a cover plate and ground plate, a commercial grade polymethyl methacrylate (PMMA) was used to provide a ground plate. A dimension of a ground plate is 15 mm × 20 mm × 2 mm (W × L × H). For a cover plate, a print circuit board (PCB) with 50 microns of thickness of copper layer was used. At the cover plate, a copper layer was wear away to provide a flow channel. The cover plate had two through holes functioned as a sample inlet and sample outlet. A diameter of both through holes was 1.5 mm. To provide a complete sensor chip, a cover plate and ground plate were attached together by using a double-coated tape. The double-coated

tape was also cut in the same shape to the copper layer of cover plate. The simply illustrate of sensor chip can be depicted as figure 3.1.

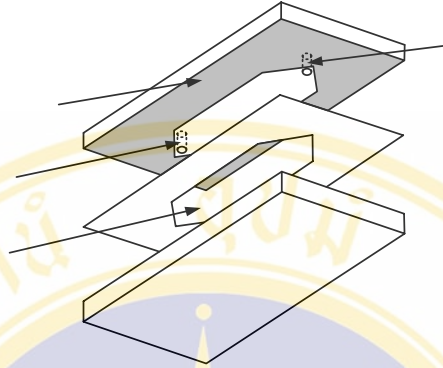


Figure 3.1 The illustration of sensor chip design.

3.1.4 Electronic devices

The side-on type photomultiplier tube (PMT) with controller model PMT-3 from optomatics USA, Inc. was used as light detector. To modulate a light source, an optical chopper model MC1000 with 10 slot blade and a controller were purchased from Thorlabs, Inc. The optical chopper had to use along with a lock-in amplifier to demodulate a signal. LIA 100 lock-in amplifier was obtained from Thorlabs, Inc. The signal from PMT was measured by using $6\frac{1}{2}$ digits agilent digital multimeter model 34401A purchased from Agilent technologies, Inc. The data from digital multimeter was acquired to personal computer by using acquisition program downloaded from agilent website.

3.2 Methods

3.2.1 Calculation

In order to fabricates a sensor chip, after the material for sensor chip fabrication was selected. The refractive index of that material was taken to calculate a critical angle of excitation beam to provide a total internally reflection by using the following equation.

$$\theta_c = \sin^{-1} \frac{n_2}{n_1}$$

3.2.2 Sample preparation

3.2.2.1 The Cyanine 5 solution

The Cyanine 5 solution was prepared by dissolving Cyanine 5 in 1 mL of Phosphate buffer saline (PBS) and mixed thoroughly. Then the Cyanine 5 solution was diluted into various concentrations.

3.2.2.2 Labeling process

Five milligrams of human albumin was dissolved in 1 mL of 0.1 M sodium carbonate buffer (pH 9.3). The protein solution was mixed thoroughly and added into the vial of Cyanine 5 dye. The solution of protein and dye were then incubated for 30 minutes with additional mixing every 10 minutes in the dark at room temperature. After the incubation, the dye-protein solution was separated from free dye by column gel filtration. The column was prepared with the filtration gel (Sephadex G50) and PBS was used as the eluting buffer. The dye-protein solution was then added into the column. Two blue bands were developed during the procedure. The faster moving band was Cyanine 5 labeled albumin solution while the slower moving band was the free dye. The Cyanine 5 labeled albumin solution was then collected and measured for the absorbance value at wavelength equal to 260 nm and 280 nm to calculate for final protein concentration. The calculation was done by using the relationship of the absorbance value of protein solution at wavelength equal to 260 nm and 280 nm as following equation.

$$\text{Concentration (mg/mL)} = (1.55 \times A_{280}) - (0.76 \times A_{260})$$

$$\text{Absorbance value at wavelength equal to 260 nm} = 0.927$$

$$\text{Absorbance value at wavelength equal to 280 nm} = 1.070$$

By substituting in the equation above, the estimation of final albumin concentration was around 954 $\mu\text{g/mL}$.

3.2.3 Immobilization of Cyanine 5 labeled albumin on sensor chip

The 20 μL of Cyanine 5 labeled albumin solution was pipetted onto the surface of ground plate or prism of sensor chip then incubated for 2 hours in the dark

at room temperature. After incubation, the exceed Cyanine 5 labeled albumin was eluted by PBS for 3 times.

3.2.4 System set up for fluorescence detection

The diode laser model LSX 635-5 was used as the light source. The laser beam was focused into the optical fiber by using objective lens. The light chopper was placed between the objective lens and the optical fiber to modulate a laser beam. At the others end of fiber optic, the laser beam was collimated by the ball lens to provide a plan wave. The laser beam was passed through others two plano-convex lenses to resize the diameter of laser into the wanted one. The laser was then strike perpendicular to the one side of prism by the angle resulting from calculation. The prism which functioned as waveguide was made by using the critical value calculated from the refractive index value of PMMA. In this design, the sensor chip was placed on the prism and the index matching gel were added between the sensor chip and prism to reduce the reflection of laser beam. The sensor chip was locked to the prism by using the holder which screwed to the based of prism. At the bottom of prism, the collector part was placed in front of the photomultiplier tube to collect and filter the fluorescence signal. The collector part consisted of two plano-convex lenses and the interference filter. The signal from the photomultiplier tube was then passed through the lock-in amplifier for demodulating and amplifying. The lock-in amplifier was connected to the digital multimeter to display. The displayed value was then stored in personal computer via the RS-232 port. In addition, the one end of the other optical fiber was placed behind the sensor chip. The other end of optical fiber was connected to the spectrophotometer to measure the spectrum of excitation and fluorescence. The simple block diagram of the primary set up can be depicted as figure 3.2.

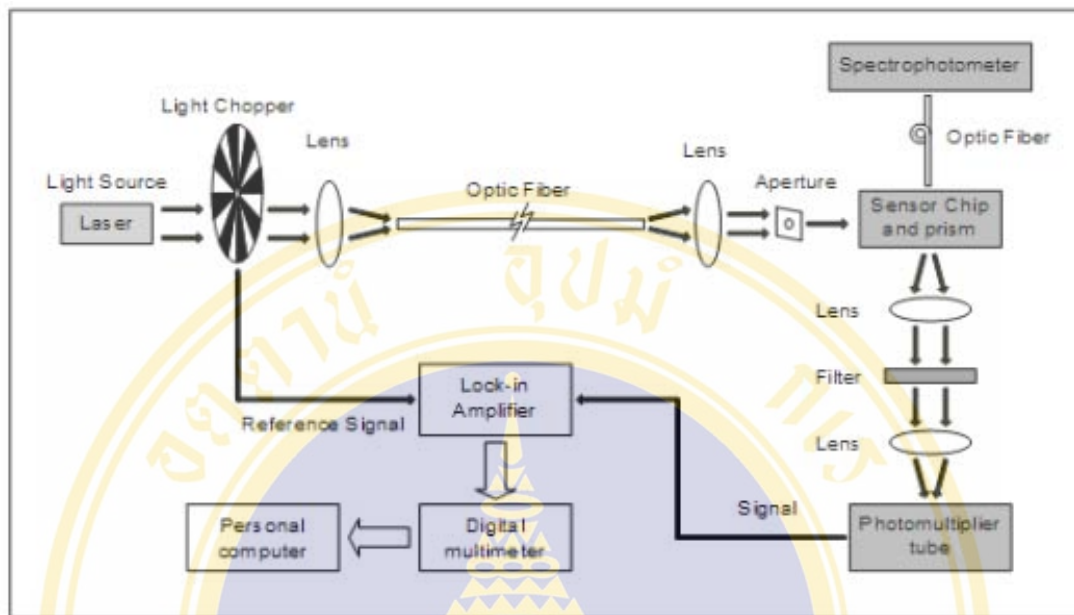


Figure 3.2 The simple block diagram of the system set up.

3.2.5 System testing

The system test for the system set up was performed by using pure Cyanine 5 solution. After the sensor chip was set on the prism, to ensure that evanescent fluorescent technique can be performed, the Cyanine 5 solution was injected into flow channel and measured for the spectrum of excitation laser and fluorescent and the intensity of fluorescent emitted from Cyanine 5. Next, the Cyanine 5 solution with different concentrations were injected to the flow channel by using concentrations ranging from 1:16 to 1:2, to check the ability in monitoring and repeatability of the system. During measurement, after one concentration of Cyanine 5 was measured, the PBS was injected to clean the flow channel and measured before the next concentration was injected. In order to prove that the evanescent could be applied to interact with the biomolecule, a kind of protein called albumin was used as a model to immobilize on the surface of flow channel. The albumin was labeled with Cyanine 5 and directly immobilized on the surface. To measure, the PBS was injected into the flow channel and starting measurement fluorescent signal. In this step, the sensor chip with sample immobilized, blank sample, and the sensor chip which only albumin immobilized were also measured to ensure that the signal measured was produced by

the emission of fluorescent from the Cyanine 5 molecule. To prove the one important characteristic of evanescent wave, surface specific, the albumin tagged Cyanine 5 was immobilized onto the cover plate and measured.

The system test in second stage was done by using the albumin labeled Cyanine 5 which diluted into various concentrations and directly immobilized on the prism. The sensor chip was placed on the chip holder in the optical module then the PBS solution was fed into the flow channel of sensor chip. After the cover of optical module was closed the measurement was started.

3.2.6 Negative control

The pure albumin was immobilized on the surface of ground plate to provide the negative control sensor chip in order to prove that the fluorescent emission was the fluorescence produced from the Cyanine 5 molecule which excited by the evanescent wave.

3.2.7 Surface specific testing

In order to prove the surface specific property of evanescent fluorescence, the albumin labeled Cyanine 5 was directly immobilized on the cover plate which the evanescent wave could not reach. The phosphate was injected into the flow channel to provide the same condition before the measure was started. The Cyanine 5 was immobilized on the location as shown in figure 3.3.

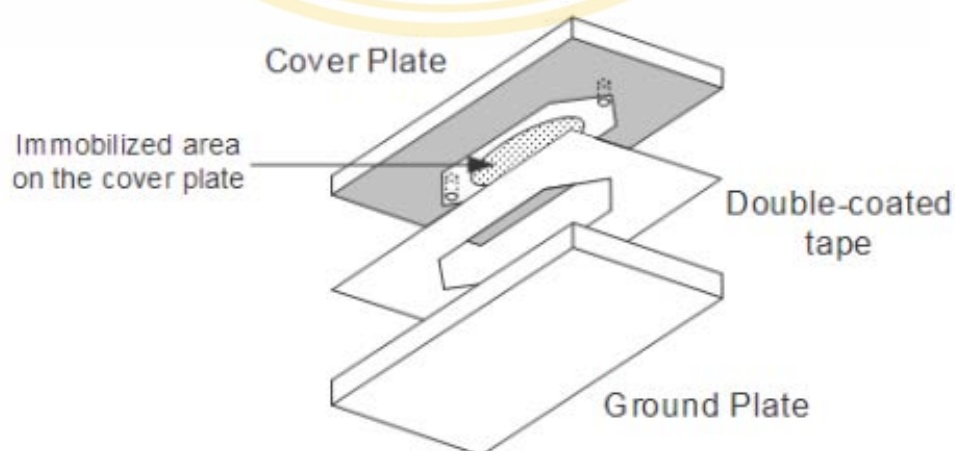


Figure 3.3 The immobilized area on the cover plate.

3.2.8 Error correction

Since a few problems occur from the system set up and sensor chip design, the system set up and sensor chip were then developed to solve those problems. In addition, the system set up was also reduced in size to more compact and ready for further development.



CHAPTER IV

RESULTS

4.1 The critical angle calculation

In order to align the system components and make the prism, the critical angle had to be calculated. The critical angle can be calculated from the following equation:

$$\theta_c = \sin^{-1} \frac{1.33}{1.49} = 63.204^\circ$$

For the ease of the prism making and component alignment, the angle at 70° was selected. In case of PMMA with $n_2 = 1.33$, $n_1 = 1.49$, $\theta_i = 70^\circ$, $\lambda_0 = 635\text{nm}$:

$$d = \frac{635 \times 10^{-9}}{4\pi \sqrt{(1.49)^2 \sin^2 70 - 1.33^2}} = 115.43 \text{ nm}$$

Calculating for d at $\theta_i = 65^\circ, 70^\circ, 75^\circ, 80^\circ, 85^\circ$ in case of PMMA:

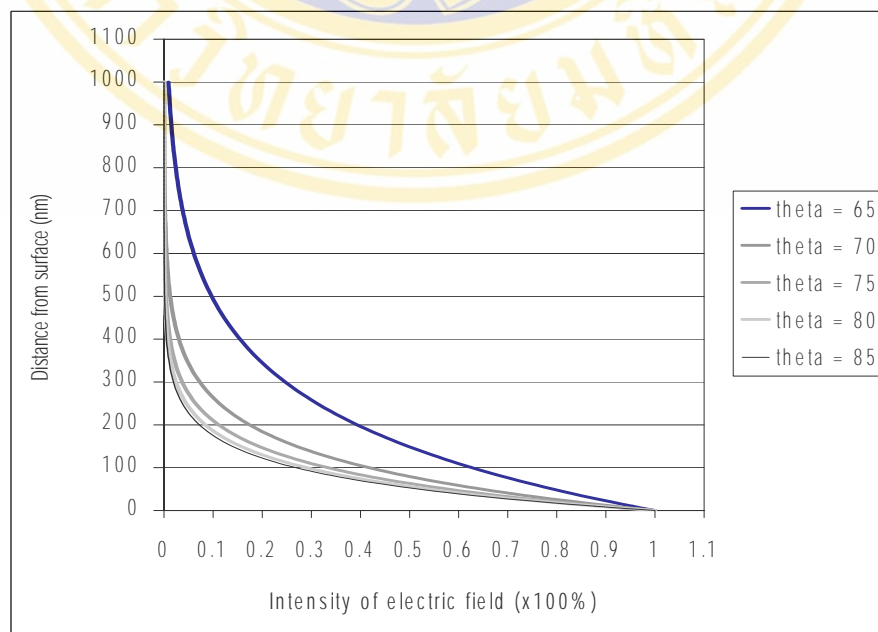


Figure 4.1 The decayed wave at different θ_i .

In conclusion, according to eq. (13) in page 8 and figure 4.1, it can be seen that the evanescent wave is a decayed wave and exponentially decay from the interface of different medium. The efficient range is calculated from the penetration depth and values about λ_0 . Thus, the advantage of using evanescent electromagnetic is that, the amplitude of this wave decays exponentially with distance into the surrounding solution, only fluorescent compounds located within range of the penetration depth from the interface will be exposed to full intensity of the radiation. Fluorophores located in solution beyond this evanescent zone will not be exposed to excitation radiation and will not fluoresce. That means the evanescent wave has a surface specific property.

4.2 The spectrum of excitation and fluorescence

In the primary set up, the spectrophotometer was added in the beginning of the experiment to check the property of Cyanine 5. The undiluted Cyanine 5 solution in PBS was used as a sample in this experimentation. The spectrum of laser source and the fluorescent emission were shown in the figure 4.2.

The lower peak was the spectrum of the laser source and the higher peak was the spectrum of the fluorescent emission. The result shown in figure 4.2 was the stroke shift effect, the property of Cyanine 5. According to the specification of Cyanine 5 from the manufacturer, the absorption peak was 649 nanometers and the peak of fluorescent emission was 670 nanometers. The spectrum obtained from the spectrophotometer was comparable to the spectrum given by the manufacturer. The comparison of between the spectrum obtained from spectrophotometer and the spectrum given from the manufacturer was shown in figure 4.2.

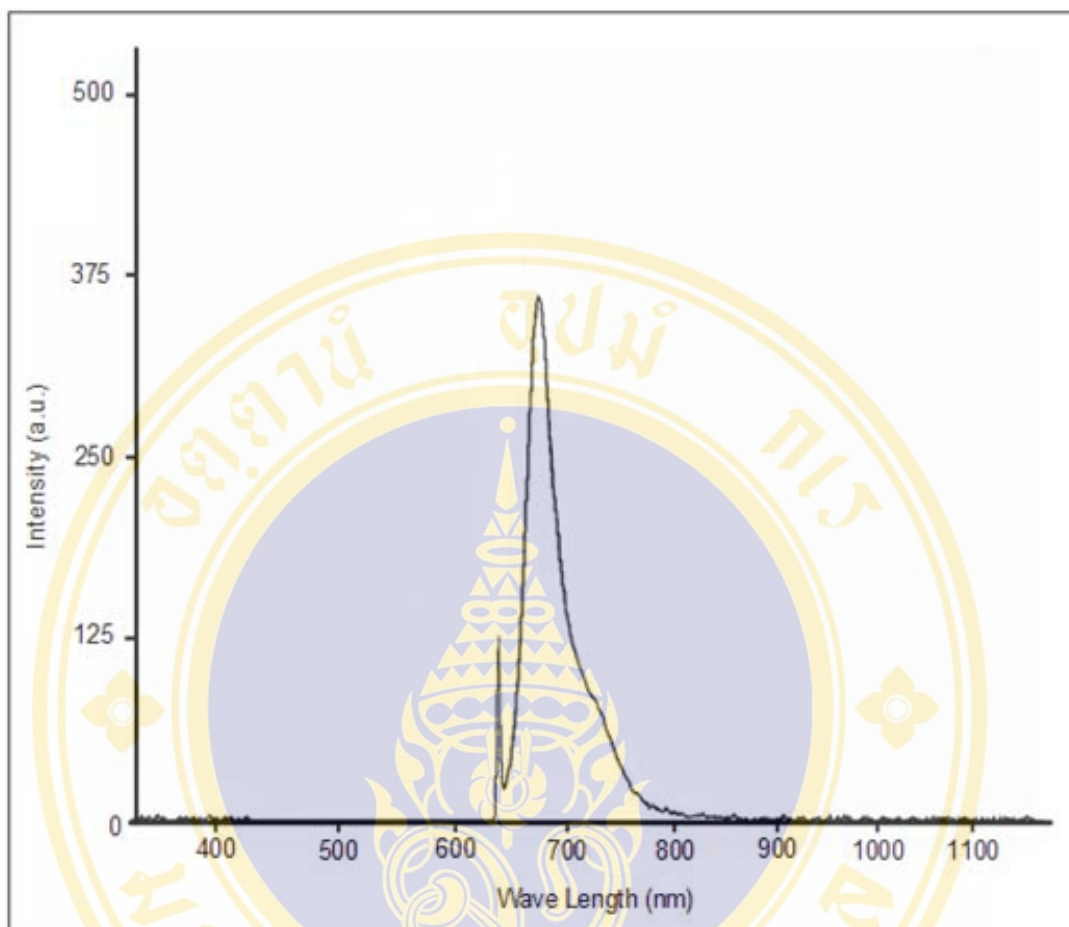


Figure 4.2 The spectrum of laser source and the spectrum of fluorescent emission.

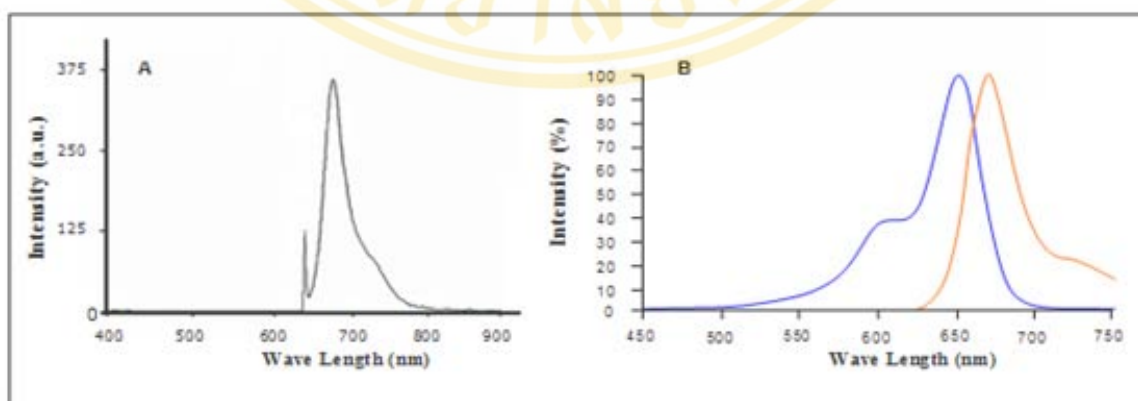


Figure 4.3 The comparison between the spectrum obtained from spectrophotometer (A) and the spectrum given from the manufacturer (B) [27]

From the comparison, it was shown that the spectrum of excitation laser and the spectrum of fluorescent wave obtained from the spectrophotometer related to the absorption range and the emission range of Cyanine 5 given from the manufacturer, respectively.

4.3 Stability of fluorescence signal

The sample used to measure a spectrum of excitation laser and the spectrum of fluorescent emission was also measured for the intensity of fluorescent emission by using photomultiplier tube. In this section of experimentation for system set up test, the laser beam was blocked by the shutter before the pure Cyanine 5 solution in phosphate buffer saline was injected into flow channel then the shutter was opened and the measurement was began. The signal of the intensity of fluorescent emission acquired by the photomultiplier tube was shown in figure 4.4.

In this experimentation, the signal detected from the undiluted Cyanine 5 solution in PBS has an average voltage signal level at 0.73 V. The voltage signal swing in then range of ± 0.01 V.

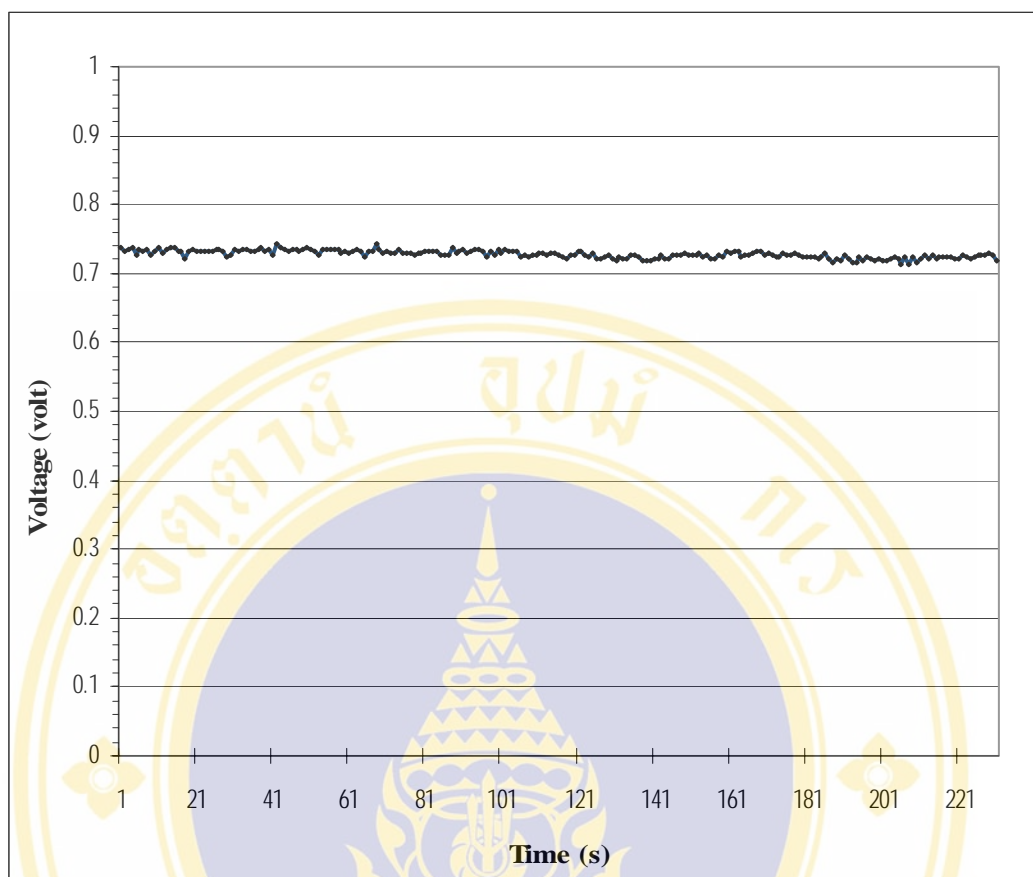


Figure 4.4 The intensity of the fluorescent emission obtained from photomultiplier tube.

The undiluted Cyanine 5 was used as a sample. The fluorescent emission was collected by the plano-convex lens before pass through the interference filter and focused by another plano-convex lens onto the sensitive area of photomultiplier tube. The voltage signal from photomultiplier tube was then displayed by digital multimeter and stored on the personal computer.

4.4 Response of the system set up to various concentration of Cyanine 5 solution in PBS.

From the result of the intensity of fluorescent, the Cyanine 5 solution in PBS was diluted into various concentrations and injected into flow channel to measure to ensure that the system set up can be used to monitor a variation of interaction of biomolecule. The Cyanine 5 solution in PBS with concentration starting from 1:16 was injected into the flow channel and measured. After measuring, before the next concentration of Cyanine 5 solution in PBS was injected, the PBS was fed to clean the flow channel to provide a base line of the signal. Then the next concentration of Cyanine 5 solution in PBS was fed and measured. The same procedure was done repeatedly until the last concentration. The signals of various concentration of Cyanine 5 solution was shown in figure 4.5.

The signals of the same concentration of Cyanine 5 solution in PBS was further calculated for an average and standard deviation value and plotted to the graph. The calibration curve of data was plotted by using the average and standard deviation value of all signals as shown in figure 4.6.

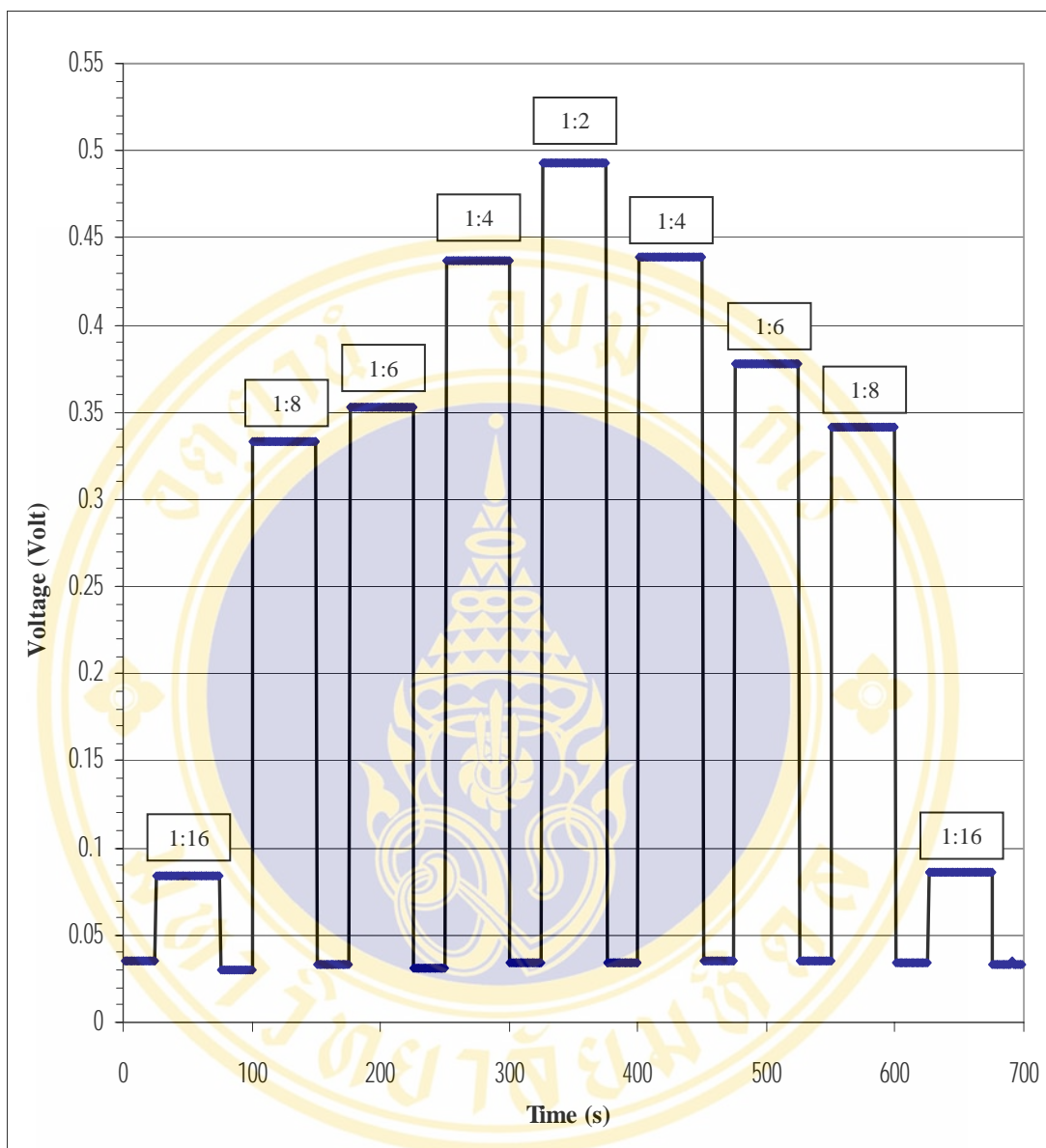


Figure 4.5 Response of fluorescent signal to the different concentration of Cyanine 5 at various measuring time.

The various concentrations of Cyanine 5 solution in PBS starting from 1:2 to 1:16 were measured. Between each concentration, the PBS was fed to clean the flow channel to provide the base line of the signal.

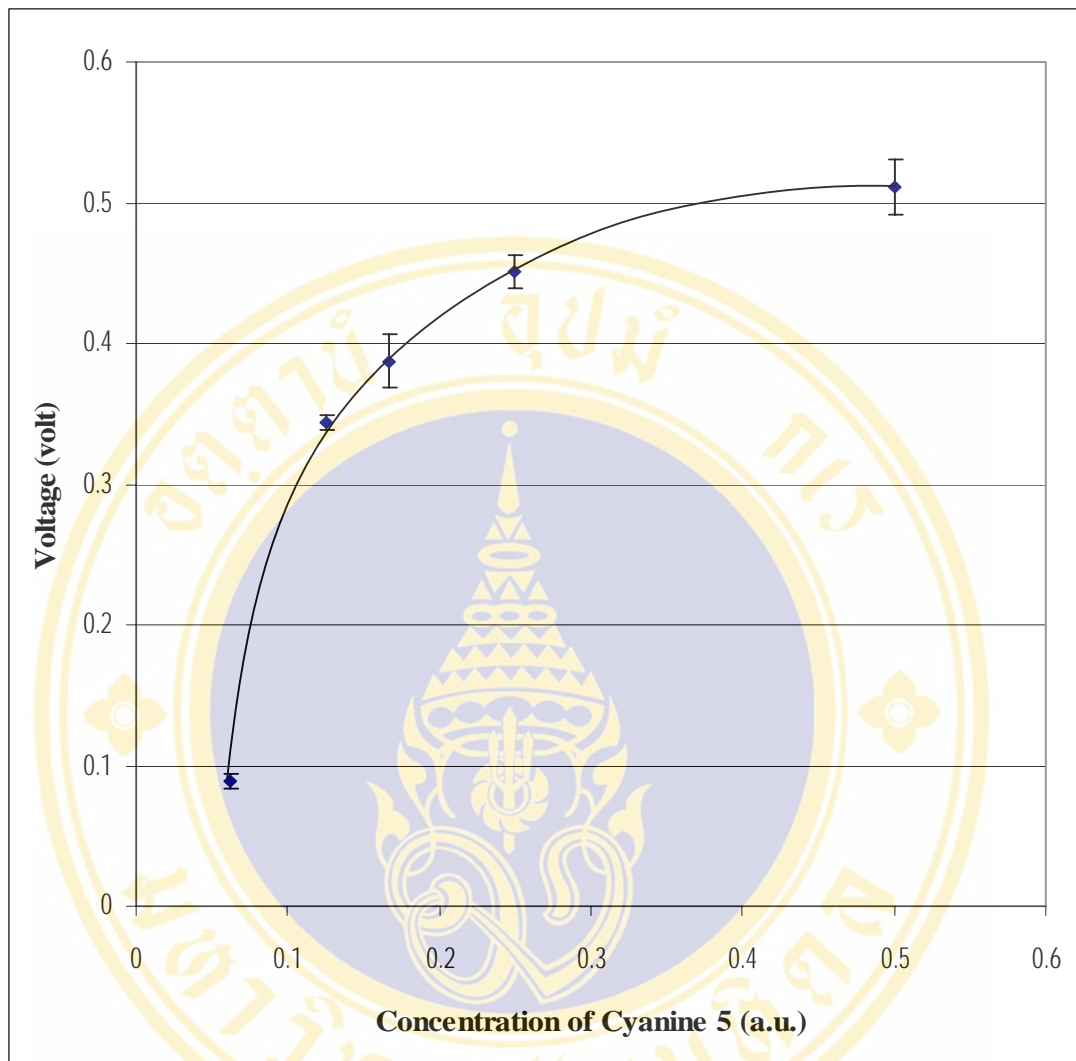


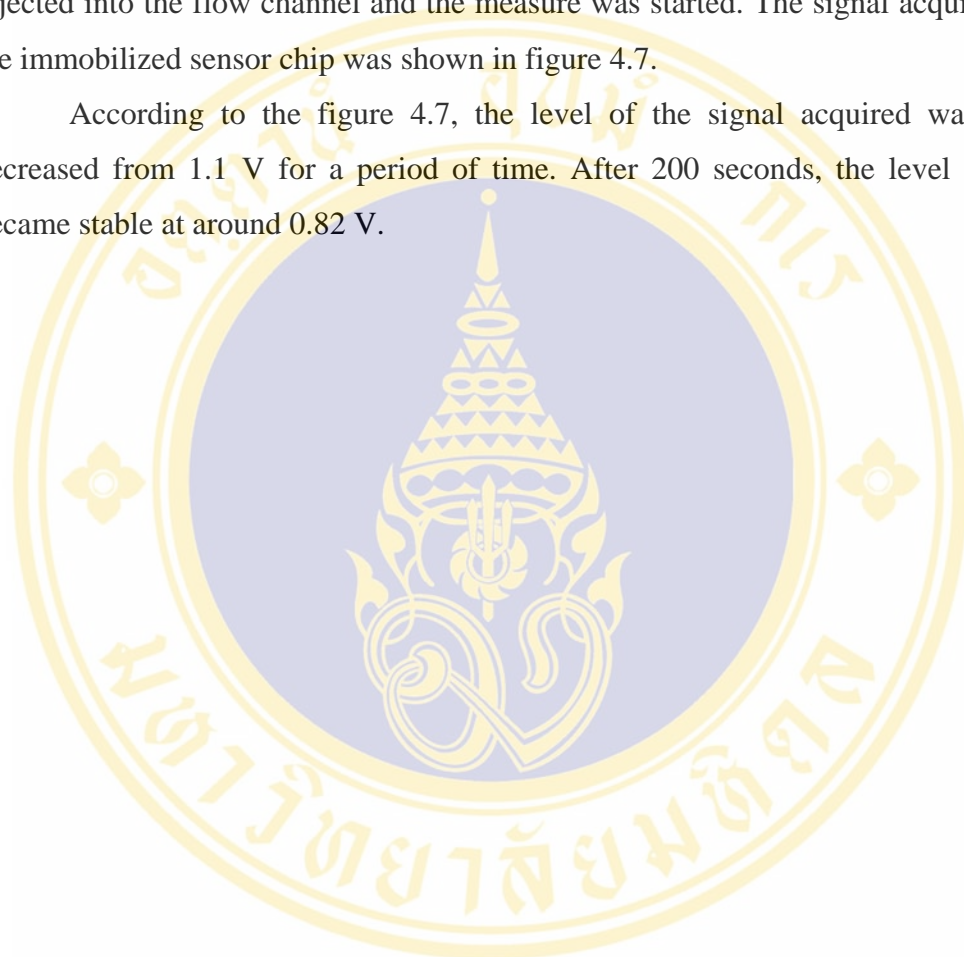
Figure 4.6 Correlation between concentration of Cyanine 5 and fluorescent signal obtained from system set up.

All voltage level of fluorescent signals obtained from the same concentration of Cyanine 5 solution in PBS were calculated for an average value and standard value and plotted into the graph. The calibration curve was plotted by using all average and standard value calculated.

4.5 Immobilized sensor chip

To stimulate the almost real interaction of biomolecular, the Cyanine 5 labeled albumin was directly immobilized onto the surface of the ground plate of sensor chip. The sensor chip was set into the system before the phosphate buffer saline was injected into the flow channel and the measure was started. The signal acquired from the immobilized sensor chip was shown in figure 4.7.

According to the figure 4.7, the level of the signal acquired was clearly decreased from 1.1 V for a period of time. After 200 seconds, the level of signal became stable at around 0.82 V.



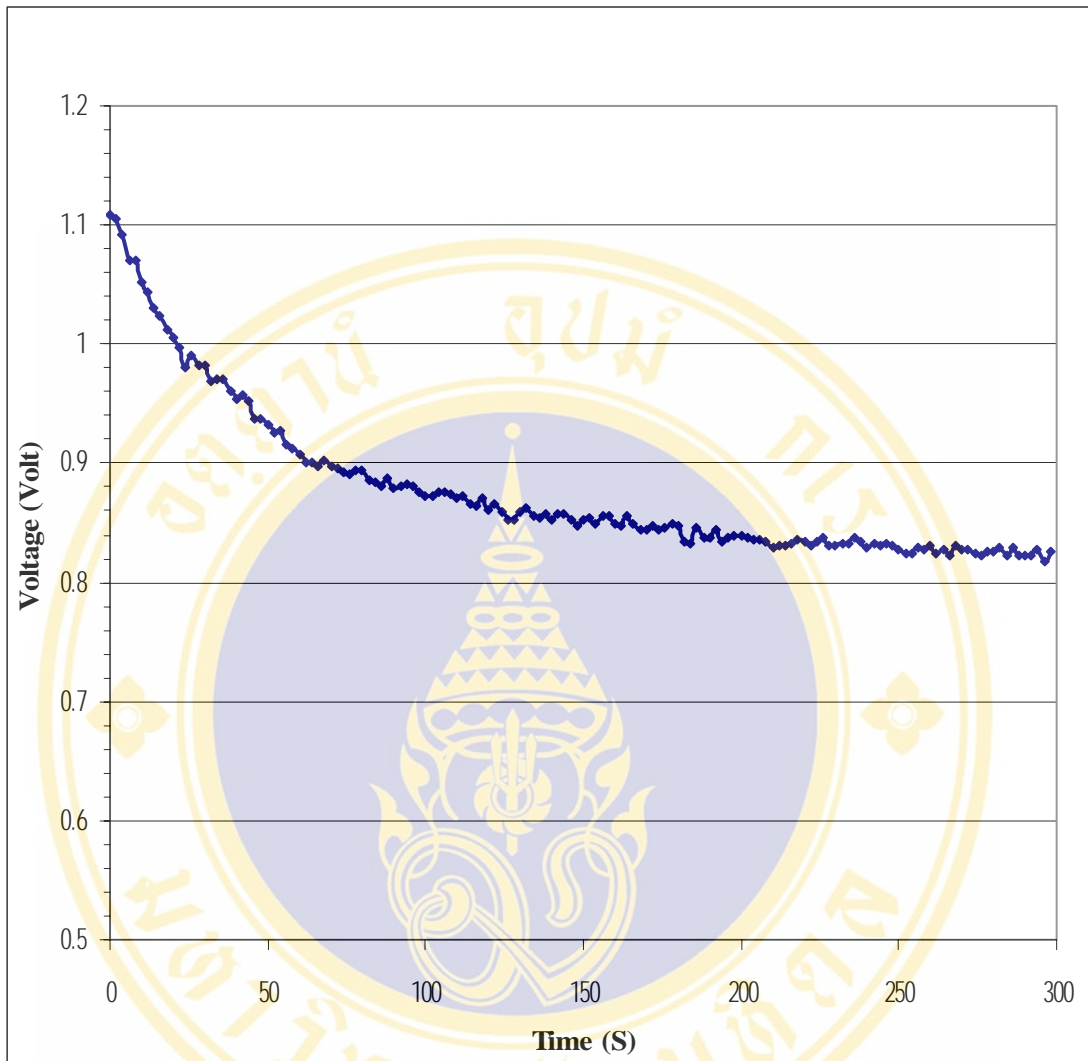


Figure 4.7 The signal acquired from immobilized sensor chip.

The 50 μL of Cyanine 5 labeled albumin solution was pipetted onto the surface of ground plate of sensor chip. After incubation for 2 hour in dark at room temperature, the exceed Cyanine 5 labeled albumin was eluted by PBS for 3 times. To measure, the PBS was fed into the flow channel to provide a same condition for the measurement.

4.6 Negative control

The signal of the blank sample which no Cyanine 5 labeled albumin immobilized on the surface of sensor chip, and the signal of negative control which only albumin immobilized on the surface of sensor chip were illustrated to compare with the signal acquired from the immobilized sensor chip in order to investigate where the fluorescent emission came from. The compared signal was illustrated in figure 4.8.

As shown in figure 4.8, the higher level signal was the signal from the Cyanine 5 labeled albumin immobilized on the sensor chip which has an average voltage signal level at 0.775 V. At the bottom of figure 4.8, there were two signals plotted together. The first signal at the bottom was a signal from the blank sample which no Cyanine 5 labeled albumin immobilized on sensor chip. The second signal was the signal from the negative control which only albumin immobilized on sensor chip. The average voltage signal level of two signals was 30 mV.

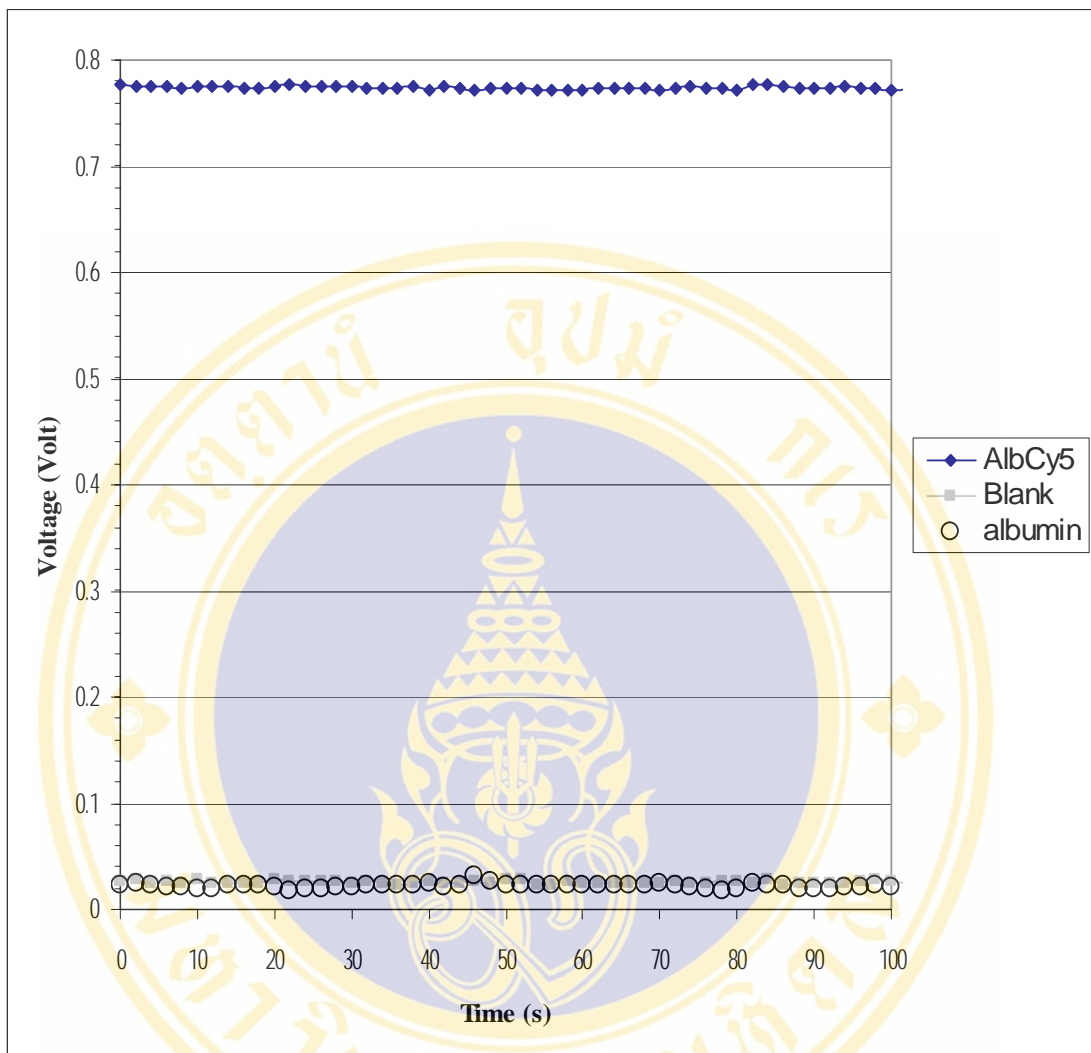


Figure 4.8 The comparison of the signal acquired from three difference sensor chip.

The signal obtained from normal sensor chip, blank sensor chip, and negative control sensor chip were plotted together to compare the level of signal. The higher one was the signal from normal sensor chip. Two signals at the bottom were the signal from blank sensor chip and negative control.

4.7 Surface specific testing

The Cyanine 5 labeled albumin was immobilized on the cover plate in order to ensure that the fluorescent emission was emitted from the Cyanine 5 molecule in range that evanescent wave can reach. The signal of Cyanine 5 labeled albumin immobilized on cover plate was depicted in figure 4.9.

According to the figure 4.9, the signal obtained from the Cyanine 5 labeled albumin immobilized on the cover plate has an average voltage signal level around 30 mV. It can clearly be seen that the voltage level of the signal was almost equal to the signal obtained from the blank sample and the negative control. The result from this experimentation shown that the Cyanine 5 molecule in the range higher than the evanescent wave can reach was not excited so the Cyanine 5 molecule in that range can not emit fluorescence which related to the surface specific property of the evanescent fluorescence theory. Although, there were a few problem occurred in the primary system set up and primary sensor chip.

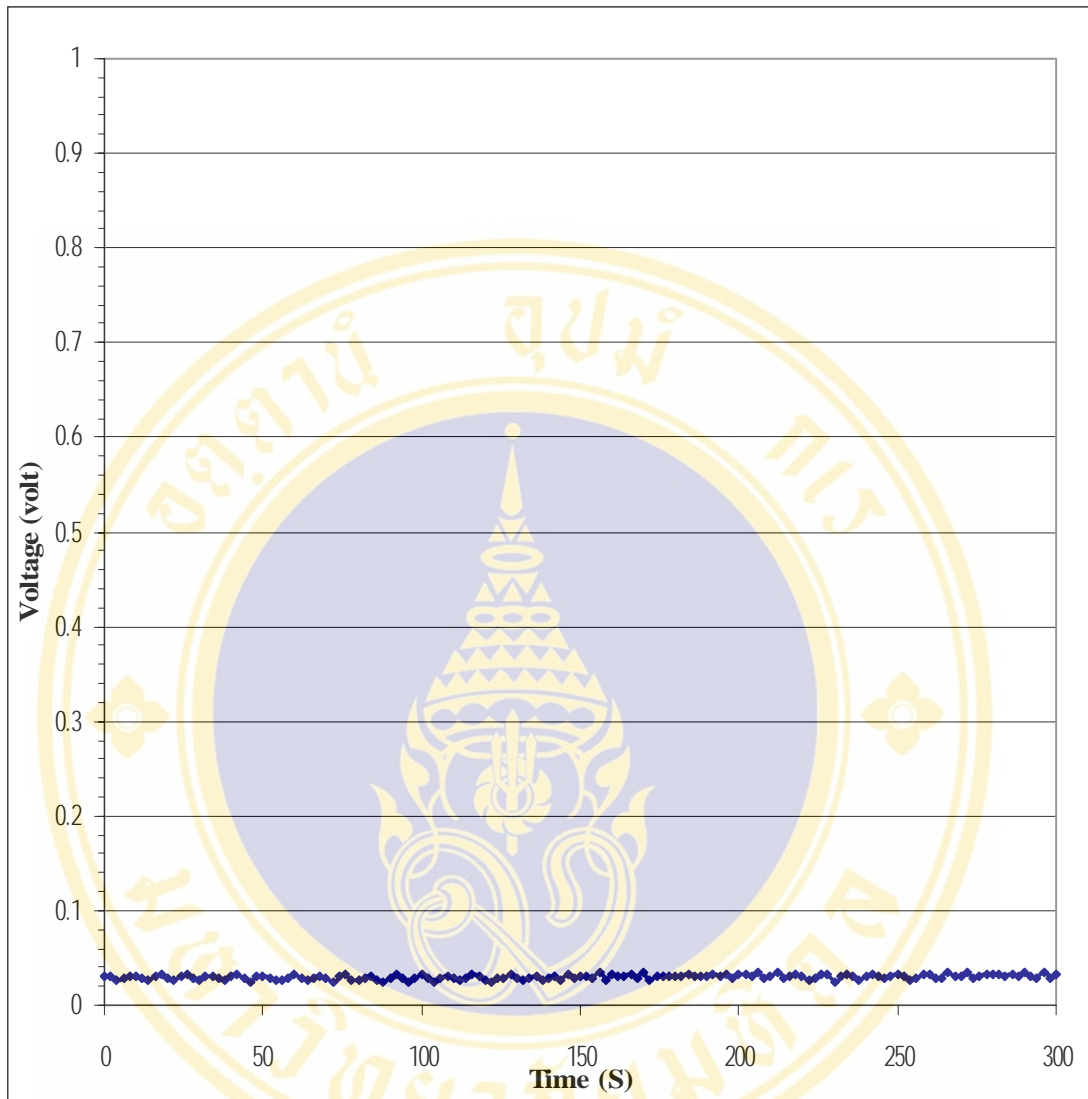


Figure 4.9 The signal of the Cyanine 5 labeled albumin immobilized on cover plate.

The Cyanine 5 labeled albumin was immobilized on the cover plate. Then the cover plate was attached to the ground plate as usual to provide a sensor chip. After the sensor chip was set into the system, the measurement was started.

4.8 Error and correction

From the primary set up, there have been a few problems occurring from the optical configuration part. The problems encountered from the primary set up were resulting from the optical post, using of index matching gel, and copper layer on print circuit board. In addition, the surrounding environment also caused the problem. The described problem led to the system redesign.

For the improve stage, the laser diode model HL3412G was replaced in stead of the old one to reduce a size of the system. The driver circuit was provided by using a simple circuit. The calculation of the component in the circuit was based on the supply current and supply voltage of laser diode. The schematic of driver circuit was shown in figure 4.10.



Figure 4.10 The driver circuit of the laser diode.

The laser beam was resized by using two plano-convex lenses before passed through the aperture and entered into the optical module. The light chopper was placed between the laser diode and the first lens to modulate the laser beam. The optical module was almost close system for a sensor chip holder, lenses and filter holder and adapter for photomultiplier tube which perpendicularly aligned in order respectively. The fluorescence were collected and focused onto the photomultiplier tube by this lenses and filter. The focus values of the lenses were calculated from the dimension of the flow channel for lens placed close to the sensor chip and from the dimension of photocathode of the photomultiplier tube for lens placed close to photomultiplier tube. The simple illustrator of the optical module was depicted in figure 4.11. The signal from the photomultiplier tube was demodulated and amplified by lock-in amplifier along with the reference signal from the light chopper. For the

data acquisition part, the same set up was used. The simply illustrate can be depicted as figure 4.12.

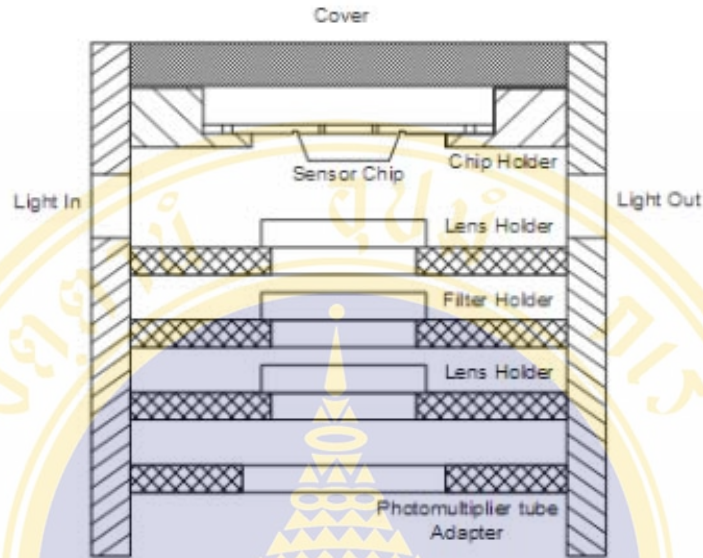


Figure 4.11 The cross-section illustrator of optical module.

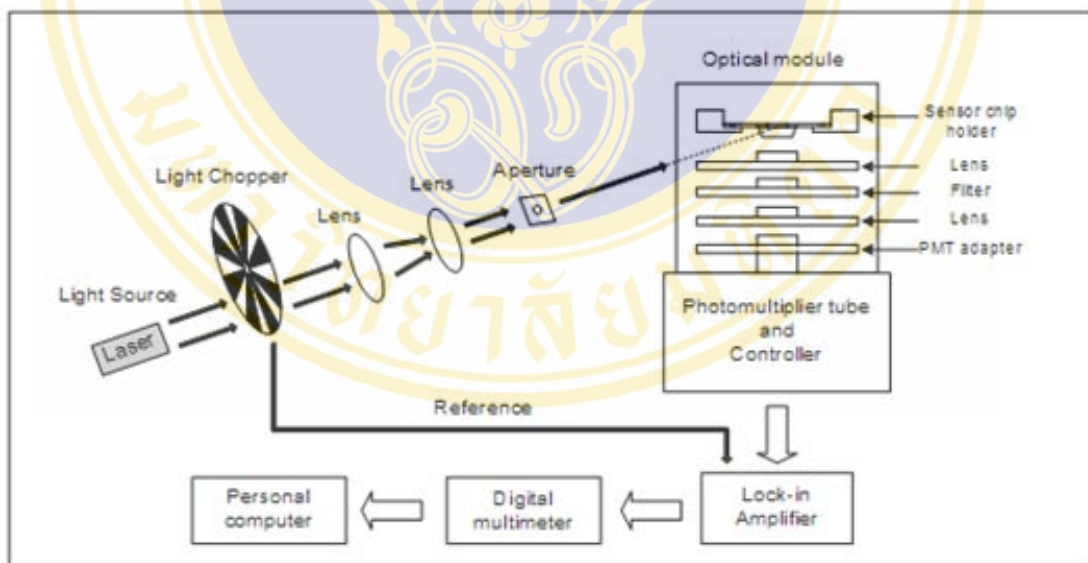


Figure 4.12 The block diagram of the developed system set up.

In order to match with the developed system and solve the problem, the sensor chip was also redesigned. The sensor chip still consisted of two components. But the shape of both two components was completely differed from the first design. For the cover plate, the print circuit board was replaced by the polymethyl methacrylate plate.

The dimension of the cover plate was changed to 15mm. × 60mm. × 2mm. (W × L × H). Beside, there were two slotted line functioned as a guide line for prism attachment to avoid mislocation. The other piece of sensor chip was prism. Prism was made in trapezoidal shape. The critical angle from the calculation was used to make a prism. The simply illustrate of developed designed of the sensor chip can be depicted as figure 4.13.

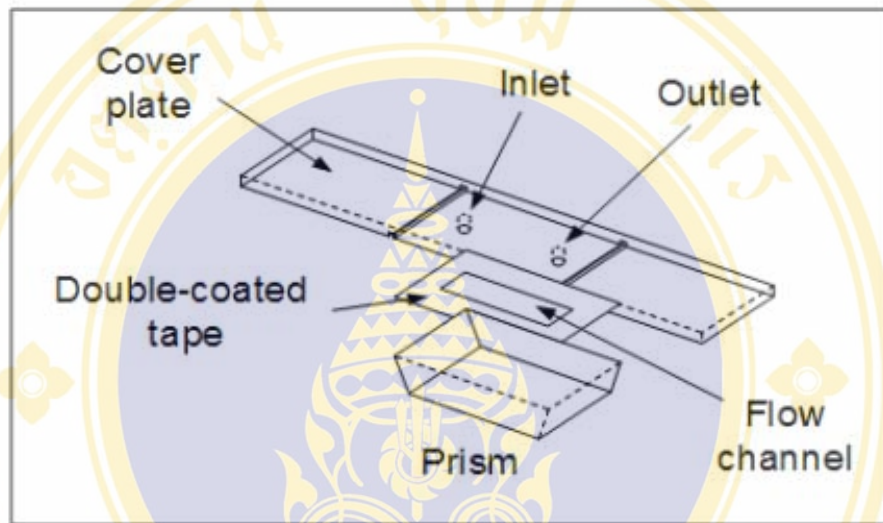


Figure 4.13 The illustrator of developed sensor chip.

4.9 Response of the developed system to various dilution of Cyanine 5 labeled albumin.

After the system set up and sensor chip have been developed, the various Cyanine 5 labeled albumin dilution were measured by using the same procedure to determine a limitation of the system. In detail, the Cyanine 5 labeled albumin was directly immobilized on the surface of the prism. The sensor chip was set into the optical module in the system in order to measure. The signal of various dilutions of Cyanine 5 labeled albumin were illustrated in figure 4.14.

As shown in figure 4.14, the signals from different dilution of Cyanine 5 labeled albumin were plotted. The signals presented in figure 4.14 were starting with undiluted shown as the highest one, then 1:4, 1:16, 1:32, 1:64, 1:128, respectively, and end up with blank at the lowest one.

The dilutions of Cyanine 5 labeled albumin of the developed system set up and sensor chip were calculated back to concentration value. The signal of each dilution was calculated for the average value and the standard deviation value. All average values of all concentrations were plotted to the graph along with the standard deviation value of each concentration. The calibration curve was added into the graph by using the average value. The average value and the deviation value were plotted in figure 4.15.

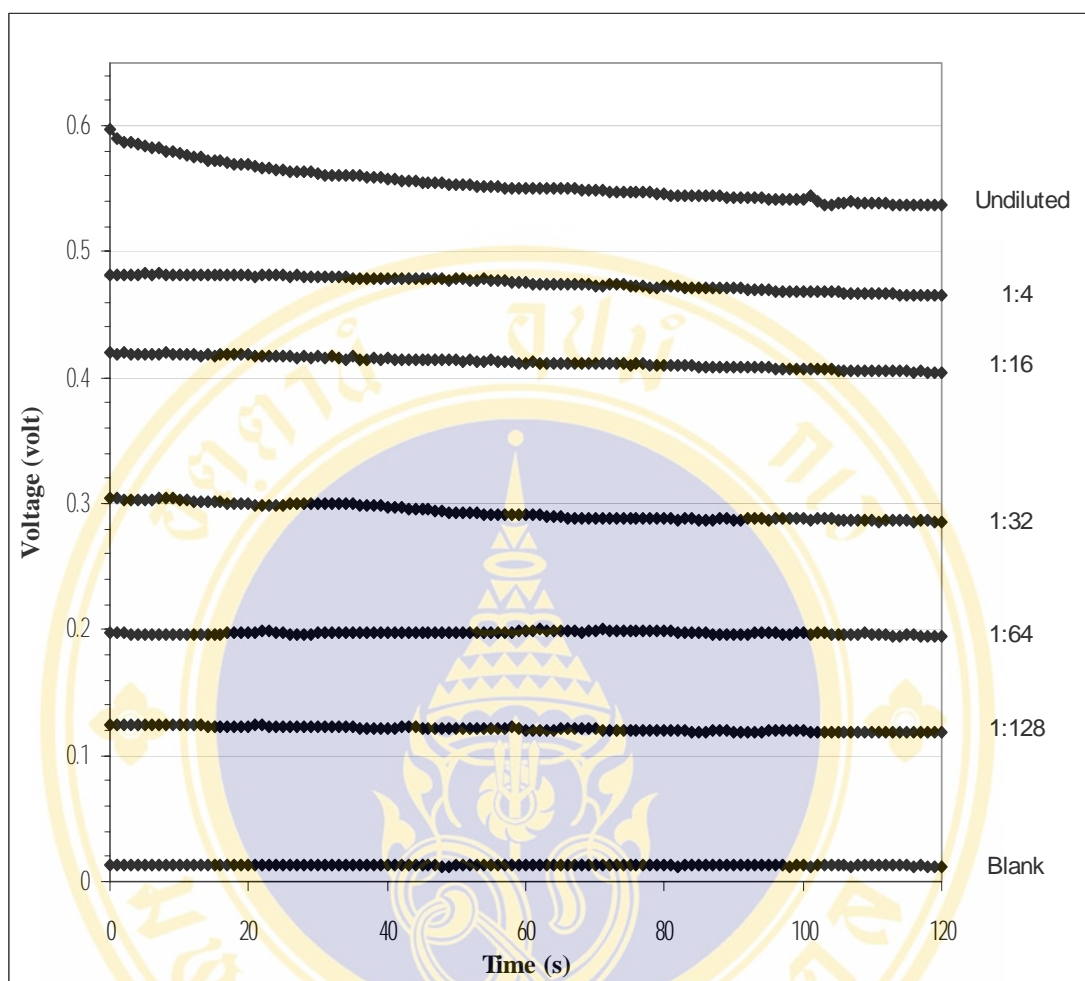


Figure 4.14 The signals of dilution of Cyanine 5 labeled albumin.

The signal of various concentration of Cyanine 5 labeled albumin immobilization starting from undiluted. 1:4, 1:16, 1:32, 1:64, 1:128, and blank were plotted together to show response of the developed system to each concentration.

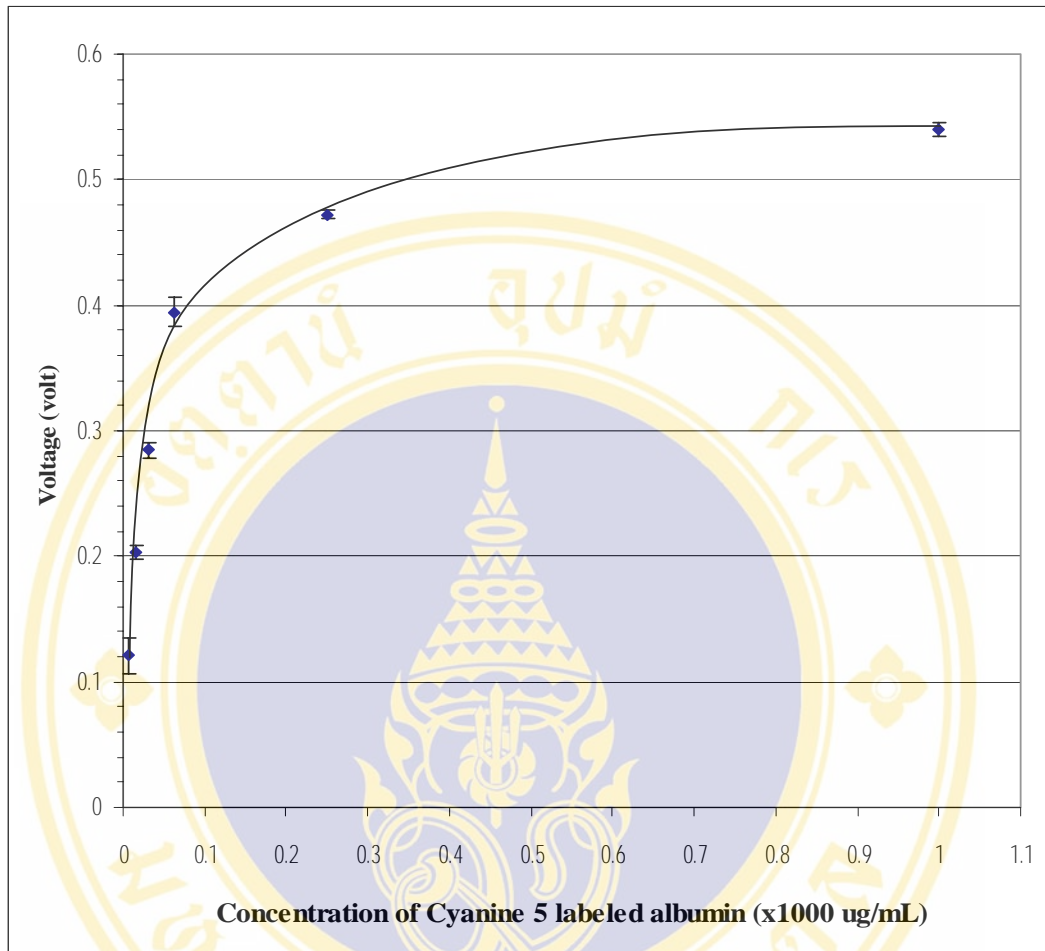


Figure 4.15 Correlation between concentration of Cyanine 5 labeled albumin and fluorescent signal obtained from developed system.

All voltage level of fluorescent signals obtained from the same concentration of Cyanine 5 labeled albumin were calculated for an average value and standard value and plotted into the graph. The calibration curve was plotted by using all average and standard value calculated.

CHAPTER V

DISCUSSION

According to the calculation for critical angle, figure 4.1 shown that the angle selection effects to the penetration depth of evanescent wave. The angle selection for the exciting laser was depended on the type and size of the sample of interest and also includes a technique used in the experimentation. For the example, in sandwich assay, the angle selection for exciting laser was depended on the summation value of size of capture antibody immobilized, analyte of interest, and tracer antibody. The range of evanescent wave has to equal or a little higher than a distance from the surface to the tracer antibody.

By using the primary system set up, after all components were aligned into the system, the signal shown in figure 4.2 was obtained from the spectrophotometer provided a corresponding curve which related to the specific characteristic curve of Cyanine 5 given from the manufacturer [27]. As shown in figure 4.2, the lower peak one was the peak of excitation laser which located in the range of the absorption wavelength of the Cyanine 5 molecule and the higher peak one was the peak of the fluorescent emission which also located in the range of the fluorescent emission wavelength of the Cyanine 5. It can be seen that the lower peak one has a very narrow spectrum width causing from the property of laser light source. And the higher peak one has a wide spectrum width since the characteristic of Cyanine 5. The graph shown that the Cyanine 5 can be functioned along with this system set up.

The signal shown in figure 4.4 was the signal of the fluorescent emission of pre-conditioned system acquired by using photomultiplier tube. The signal of fluorescent emission was used to condition the output signal from photomultiplier tube by adjusted the controller of photomultiplier tube to provided a proper level of signal. After conditioned, the signal with various concentration were measured, the result of the experimentation was shown in figure 4.5. The signal shown in figure 4.5 indicated that the system set up can be monitored a change of level of signal, in others

hand, a change in concentration. The signal in figure 4.5 also had shown the repeatability of the system. As described previously, between the signals of concentration, the phosphate buffer saline was fed into the flow channel to wash the flow channel and provided the base line (background) of the system. It can clearly be seen that the background signal always back down to the same level of voltage. However, the problem of the system set up can be discovered from the result of experimentation. Since the level of each dilution should be equal or almost equal to each other. But some dilutions were differing in level in each measurement. The problems encountered from a few reasons. The first one was the sensor chip holder. The sensor chip holder in primary set up was the prism which placed on the magnetic post. The magnetic post can be rotated in vertical axis resulting from too much force applied initiating in misposition of the laser beam. The second one was the matching gel which used to reduce the reflection of laser beam. The matching gel used in primary set up could possibly interacted with PMMA caused the enormous scratch on the surface of prism which reduced the long term use of prism. The third problem causing from the sensor chip itself, the edge of copper layer of the cover plate could reflect the scattering laser illuminated on desired area. The surrounding light was another cause of problem in primary system set up. Since primary system set up was cover by nothing, the surrounding light could possibly effect to the level of signal and background level.

In figure 4.7, the Cyanine 5 labeled albumin was immobilized on the surface of the ground plate of sensor chip to simulate the biological reaction. The level of the signal acquired was clearly decreased for a period of time after the buffer injection due to the excess Cyanine 5 labeled albumin on the surface dissolved into the solution which evanescent wave can not reach. After period of time, the signal became stable. This can also be used to explain the different of the starting level of the signal between figure 4.7 and figure 4.4.

To investigate the source of the fluorescent emission, the three sensor chips with difference sample immobilization were provided. The primary sensor chip was the normal one, the Cyanine 5 labeled albumin was immobilized on the surface of ground plate of sensor chip. The developed sensor chip was the blank sensor chip, there was nothing immobilized on the surface of ground plate of sensor chip. The

third one was the negative control sensor chip, there was only albumin immobilized on the surface of ground plate of sensor chip. The signal of three sensor chip were plotted to compare in figure 4.8. The higher level signal on the top of the graph was the signal from the primary sensor chip. At the bottom of the graph, there were two signal plotted together, the signal of blank sensor chip and the signal of negative control. It can clearly be seen that, the signal of the blank sensor chip and the signal of negative control were almost equal. The comparison of three signals provided a strong enough evidence to believe that the fluorescent acquired was the fluorescence emitted from the Cyanine 5 molecule excited by the evanescent wave, not from the albumin molecule or phosphate buffer saline.

Another important property of evanescent fluorescence, the advantage of evanescent fluorescence over the others, is the surface specific. The next experimentation was set to ensure that the system set up can perform the surface specific property. As described previously, the Cyanine 5 labeled albumin was immobilized on the cover plate of the sensor chip. The signal obtained was shown in figure 4.9. The level of the signal obtained was equal to the blank sensor chip. From the result of the experimentation, it can be concluded that the fluorescence was the emission of the fluorophore molecule in the range that evanescent wave can be reached.

All results obtained from the experimentation of primary system set up led to one conclusion which is the system set up can be performed as the evanescent fluorescence monitoring system.

Initiating from the result in primary sensor chip design and system set up which causing the problems, the sensor chip was redesigned and the system set up was developed. For the sensor chip, the printed circuit board was replaced by the same type of polymethyl methacrylate plate. The ground plate was replaced by the prism produced from the same material with the cover plate. The details of the new sensor chip were described in chapter IV. For system set up, the laser diode was replaced by another model, the optical fiber was abandoned causing from the new laser diode. The collector part which consists of sensor chip holder, two lenses, interference filter, and photomultiplier adapter was united into the optical module to avoid surrounding light. The details of developed system set up were also described in

chapter IV. After primary system set up was developed, the experiment for system testing was preformed.

The experiment for developed system set up began with the Cyanine 5 labeled albumin solution was diluted into various concentrations then directly immobilized onto the surface of prism. The signals of various dilutions were plotted in figure 4.13. According to figure 4.13, the level of background signal was around 16 mV. While the level of background signal of primary system set up was around 30 mV. And, in developed system set up, the lowest limitation of the system set up equal to 1:128 while equal to 1:16 for primary system set up. Then, the dilutions of Cyanine 5 labeled albumin solution were calculated back to concentration. The average value and the standard deviation of each concentration were calculated and plotted into figure 4.14. The calibration curve was added to the graph by using the average value. According to the figure 4.14, it can be seen that the concentration of Cyanine 5 labeled albumin at around 8 $\mu\text{g/mL}$ can be detected by the system set up.

The results from the experiment in developed system set up shown that the developed system set up had more efficiency and lower background level then the primary one. However, the developed design of sensor chip still had a little problem with the prism making process. Since the prisms were a hand-made product, so they were not perfectly same to each others resulting in irregular background signal. In addition, the optical module in developed system set up can be further developed in order to reduce the background and noise of the signal. Since the optical module was made from the aluminum which cause light reflection, black anodize coating should be applied in order to reduce the reflection of light inside the optical module.

CHAPTER VI

CONCLUSION

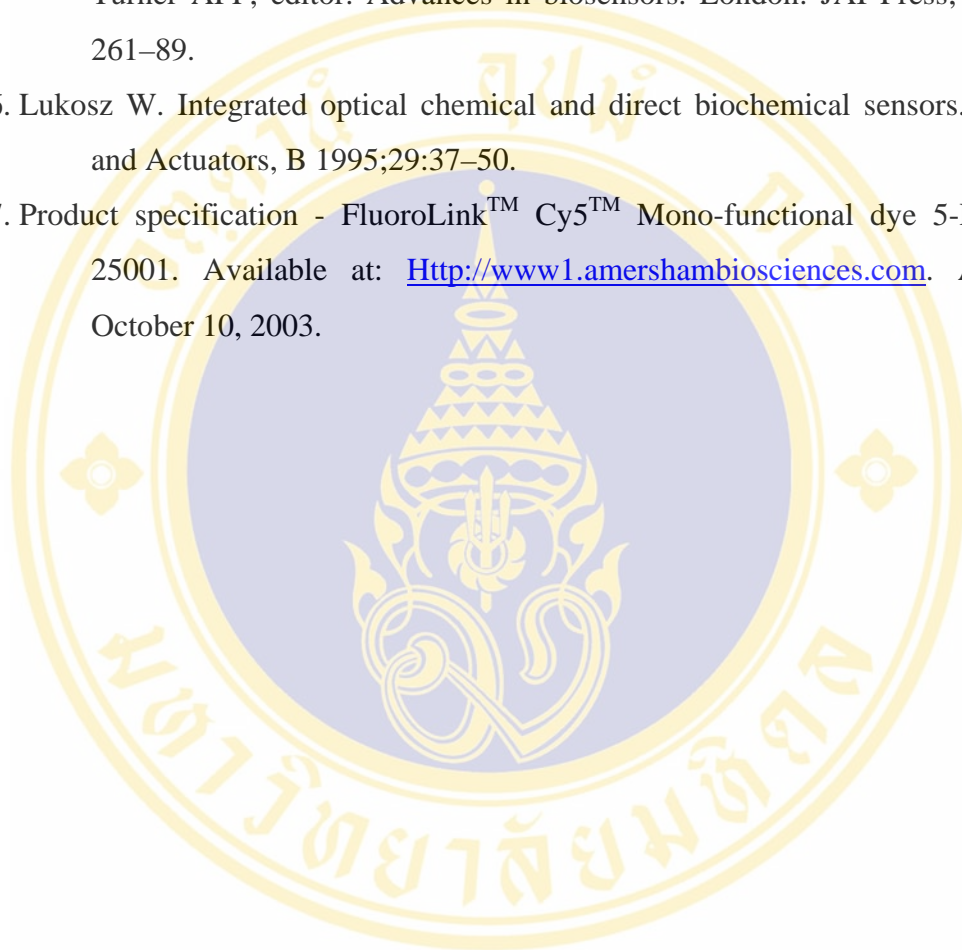
1. The total internal reflection system for biomolecular interaction monitoring was demonstrated
2. The lowest limit of the system set up was about 8 $\mu\text{g/mL}$ of directly Cyanine 5 labeled albumin immobilized on the surface.
3. The penetration depth of this system set up was 115.43 nm from the surface.
4. The system can be further developed to operational system for biomedical application.

REFERENCES

1. Meusel M, Trau D, Katerkamp A, inventor; Institut für Chemo- und Biosensorik Munster e.V., Assignee. Device and method for carrying out fluorescence immunotests. USA patent 6,686,208. 2003.
2. Carniglia CK, Mandel L, Drexhage KH. Absorption and emission of evanescent photons. *Journal of the Optical Society of America, A* 1972;62:479-86.
3. Jordan CE, Corn RM. Surface plasmon resonance imaging measurements of electrostatic biopolymer adsorption onto chemically modified gold surfaces. *Analytical Chemistry* 1997;69(7):1449-56.
4. Bier FF, Scheller FW. Label-free observation of DNA hybridization and endonuclease activity on a waveguide surface using a grating coupler. *Biosensors and Bioelectronics* 1996;11(6/7):669-74.
5. Morhard F, Pipper J, Dahint R, Grunze M. Immobilization of antibodies in micropatterns for cell detection by optical diffraction. *Sensors and Actuators B* 2000;70:232-42.
6. Tiefenthaler K, Lukosz W. Sensitivity of grating couplers as integrated-optical chemical sensors. *Journal of the Optical Society of America, B* 1989;6:209-20.
7. Wise DL, Wingrad LB. *Biosensors with Fiberoptics*. New Jersey: Humana Press Inc; 1991.
8. Keiser G. *Optical Fiber Communications*. 2nd ed. Singapore: McGraw-Hill; 1991.
9. Serway RA. *Physics for scientist and engineers*. 3rd ed. Saunders College Publishing; 1992.
10. Introduction to Fluorescence Techniques. Available at:
[Http://probes.invitrogen.com/handbook/sections/0001.html](http://probes.invitrogen.com/handbook/sections/0001.html). Accessed November 20, 2003.

11. Improving a Vibrating Sample Magnetometer. Available at:
[Http://members.aol.com/RudyHeld/index.html](http://members.aol.com/RudyHeld/index.html). Accessed December 22, 2003.
12. What is Lock-in amplifier?. Available at: www.signalrecovery.com. Accessed January 9, 2004.
13. Exploration of a Photomultiplier tube. Available at:
www.davidgilson.co.uk/academic/labreports/rep3/PMT.html.
Accessed January 27, 2004.
14. Construction and operating characteristics. Available at: www.hamamatsu.com.
Accessed March 8, 2004.
15. Module 1-1 Elements and operation of a laser. Available at:
[Http://repairfaq.ece.drexel.edu/sam/CORD/leot/course01_mod01/mod01-01.html](http://repairfaq.ece.drexel.edu/sam/CORD/leot/course01_mod01/mod01-01.html). Accessed September 2, 2004.
16. How laser work. Available at: [Http://science.howstuffworks.com/laser5.htm](http://science.howstuffworks.com/laser5.htm).
Accessed August 26, 2004.
17. Laser principle. Available at: [Http://www.ilt.fraunhofer.de/default.php](http://www.ilt.fraunhofer.de/default.php). Accessed August 29, 2004.
18. Lippa PB, Sokoll LJ, Chan DW. Immunosensors-principles and applications to clinical chemistry. *Clinica Chimica Acta* 2001;314:1–26
19. Liedberg B, Nylander C, Lundström I. Biosensing with surface plasmon resonance - how it all started. *Biosensors & Bioelectronics* 1995;10:i-ix
20. Wood SJ. DNA-DNA hybridization in real time using BIAcore. *Microchemical Journal* 1993;47:330-7.
21. Anderson GP, Rowe-Taitt CA, Ligler FS. RAPTOR: A portable, automated biosensor. In: *First Conference on Point Detection for Chemical and Biological Defense*; 2000 October; Washington DC; 2000.
22. Anderson GP, Nerurkar NL. Improved fluoroimmunoassays using the dye Alexa Fluor 647. *TRENDS in Cell Biology* 2001;11(7):298-303.
23. Block MJ, Lackie SJ, Glass TR, inventors; Block MJ, assignee. Immunoassay apparatus. USA Patent 4,990,990. 1990.

24. Herron JN, Charistensen DA, Pollak VA., McEachern RD, Simon EM, inventors; University of Utah Research Foundation, assignee. Lens and associatable flow cell. USA Patent 6,611,634 B2. 2003.
25. Tiefenthaler K. Integrated optical couplers as chemical waveguide sensors. In: Turner APF, editor. Advances in biosensors. London: JAI Press; 1992. p. 261–89.
26. Lukosz W. Integrated optical chemical and direct biochemical sensors. Sensors and Actuators, B 1995;29:37–50.
27. Product specification - FluoroLink™ Cy5™ Mono-functional dye 5-Pack PA 25001. Available at: <http://www1.amershambiosciences.com>. Accessed October 10, 2003.



BIOGRAPHY

NAME	Mr.Chotchawal Wongmahasiri
DATE OF BIRTH	23 November 1976
PLACE OF BIRTH	Bangkok, Thailand
INSTITUTIONS ATTENDER	Mahanakorn University of Teshnology, 1995 : Bachelor of Engineering (Telecommunication Engineering) Mahidol University, 2000 : Master of Engineering (Biomedical Engineering)
HOME ADDRESS	226/12 Sathupradit Rd., Bangkok 10120 Tel. 01-6151941